ELSEVIER

Contents lists available at ScienceDirect

Transportation Research Part B

journal homepage: www.elsevier.com/locate/trb



Car-following behavior characteristics of adaptive cruise control vehicles based on empirical experiments



Tienan Li^a, Danjue Chen^{a,*}, Hao Zhou^b, Jorge Laval^b, Yuanchang Xie^a

- ^a Civil and Environmental Engineering, University of Massachusetts, Lowell, United States
- ^b Civil and Environmental Engineering, Georgia Institute of Technology, United States

ARTICLE INFO

Article history: Received 1 January 2021 Revised 19 February 2021 Accepted 5 March 2021 Available online 30 March 2021

Keywords: Automated vehicles Adaptive cruise control Oscillation amplification and dampening Car-following

ABSTRACT

Emerging automated vehicle (AV) technologies are increasingly being deployed around the world and it is only a matter of time before the transportation landscape changes dramatically. Unfortunately, those changes cannot be well predicted due to the lack of empirical data. But adaptive cruise control (ACC) vehicles are common in the market and can be used to fill this gap. In this paper, we aim to characterize the empirical car-following behaviors of a commercial ACC system and understand how ACC behaves in different conditions and the underlying impact mechanism. It is found that for a single ACC: (i) the ACC response time is comparable to human drivers but much larger than the ACC controller time gap and it exhibits small variance, (ii) the ACC response can amplify or dampen an oscillation, (iii) after the oscillation, the stabilization process can exhibit overshooting or undershooting, and (iv) these CF behaviors depend largely on the ACC headway setting, speed level, and leader stimulus, which produce the impacts directly and/or indirectly through the mediation of earlier ACC behaviors. For a three-vehicle platoon, our main finding is that the change from one ACC vehicle to the next is progressive for oscillation growth, and regressive for deceleration, acceleration, and overshooting. This implies that in long platoons, oscillation amplitude tends to exacerbate very quickly, which forces ACC vehicles further upstream to apply very strong braking followed by a strong acceleration. This can cause significant overshooting and safety hazards.

© 2021 Elsevier Ltd. All rights reserved.

1. Introduction

Emerging automated vehicle (AV) technologies are here to stay, and there is general consensus that they will have particularly profound impacts on urban congestion. Since the future of AV technologies is highly uncertain and empirical evidence is lacking, the scientific community does not have a strong foundation to predict their impacts. This is causing confusion and conflicting results in the literature. But Adaptive Cruise Control (ACC), a precursor of AV technology, is now common in the market (existing in more than 20 car makers Wikipedia, 2020) and can be used to fill this gap. There is already a significant proportion of vehicles on the road equipped with ACC (about 5% in newly sold cars) and the proportion is steadily growing (Kyriakidis et al., 2015). Moreover, ACC is very likely to remain as the basic longitudinal control component for higher-level automation. Therefore, ACC is assuredly a stepping stone towards AV technologies in the future. It is therefore critical to have a thorough understanding on the behaviors of the current ACC systems. To serve the purpose, it is important to build

E-mail address: danjue_chen@uml.edu (D. Chen).

^{*} Corresponding author.

the analysis based on field experiments. There are several reasons. Firstly, controllers of commercial ACC vehicles are proprietary and not available to the public. Moreover, it is very likely that the actual ACC behaviors on road are not exactly the same as the controller design, which can be impacted by many factors, such as sensing errors and delays. Eventually, we are interested in understanding the similarity and difference of the actual ACC behaviors across different brands. So we can better predict the impacts of the general ACC population on traffic flow.

Although ACC vehicles have become common on the road, the literature only has a few efforts that examined the ACC behaviors grounded on empirical data. Regarding the string stability of ACC systems, some studies (Naus et al., 2010a; 2010b; Bu et al., 2010; Ploeg et al., 2011) have tested factory production ACC for comparing new controllers. Specifically, Naus et al. (2010b) conducted experiments on two Citroen C4s cars and showed that their cooperative adaptive cruise control (CACC) controller can achieve string stability in a larger parameter domain than the factory ACC. Similar findings were obtained in Naus et al. (2010a) and Ploeg et al. (2011) where experiments were conducted on six Prius III Executive. Bu et al. (2010) conducted tests on two Infinity FX45s and found that the factory ACC has large time gap variation, suggesting potential loss of string stability. Milanés et al. (2013) and Milanés and Shladover (2014) found that the ACC system on Infinity M56s cars could amplify disturbances especially when an ACC car is at the tail of a multi-ACC car platoon. Notably, since these studies were designed for the validation of new controllers, the tests revealed only partial information of the ACC systems, e.g., at one specific time gap setting or in a small range of speed. Moreover, a detailed analysis of the ACC systems was missing.

Naturalistic driving studies involving ACC vehicles have also been conducted. Fancher (1998) involved 108 participants to test a new ACC system and found that drivers tend to change their driving style under ACC mode. Alkim et al. (2007) and Viti et al. (2008) involved 20 Volkswagen Passats (equipped with ACC) for six-month driving, and found that the speeds and headway variance are sensibly lower with ACC active, but that the average headway increases. Schakel et al. (2017) conducted a study with eight participants using four different ACC car models and found that ACC increases spacing and time headway in saturated conditions compared to human driving, suggesting a potential capacity decrease. They also found that acceleration has a smaller variation when ACC is active. Notably, in these studies, the driving behavior analysis was conducted at the aggregate level. For example, Schakel et al. (2017) compared the spacing difference (with ACC on and off) by considering the average spacing value across all drivers. Thus, while these studies are valuable, they still could not provide a complete picture of the characteristics of ACC systems.

More empirical experiments have emerged in recent years. Researchers from the Netherlands (Knoop et al., 2019) set up a platoon consisting of seven ACC vehicles (from four different car makers) to drive on public roads for a 500 km trip. It was concluded that the long ACC platoon cannot be persistently maintained on public roads due to the aggressive lane-changing of surrounding human-driven vehicles (HDVs). Moreover, when the platoon is longer than three to four vehicles, the ACC system becomes unstable and leads to collision risks in oscillation conditions (i.e., acceleration followed by deceleration).

It is worth noting that, some pioneering efforts have been conducted with more sophisticated controlled experiments recently to understand the ACC behaviors. Gunter et al. (2020a) tested an ACC model with a set of experiments considering different settings to calibrate the optimal velocity CF model (Bando et al., 1995). The fitted model indicated that the tested ACC system was string unstable. Another test (Gunter et al., 2020b) was conducted with seven different ACC car models (from two car makers) with a similar experiment setting, and it was found that all seven models were string unstable. Moreover, one run with a seven-ACC platoon (all identical ACC) found that each ACC vehicle in the platoon exhibited a progressively more extreme braking response, illustrating the string instability feature. The two studies (Gunter et al., 2020a; Gunter et al., 2020b) mainly focused on ACC string stability from a control theory perspective. Another important milestone is the ACC campaign of the Joint Research Centre (JRC) of European Commission, which has conducted four sets of ACC experiments (Makridis et al., 2020a). Specifically, Makridis et al. (2019b) tested one ACC vehicle and estimated the response time (0.8-1.2 s) and time headway. Makridis et al. (2019a) tested two more ACC car models and found that the ACC response time was comparable to human drivers or even higher. The test in He et al. (2020) had a primary focus on energy efficiency. It used a 5-vehicle mixed platoon, with HDVs for the head and tail vehicles and 3 ACC cars (in different models) in between. It was found that the mixed platoon was unstable. Makridis et al. (2020b) tested a 5-ACC platoon (all different ACC car models) to estimate the response time (1.7 s-2.5 s) and time headway, and test platoon stability under different speed and perturbation magnitude. It was found that the platoon was unstable in all perturbation events. The serial JRC efforts have revealed some basic features of ACC and provided particularly valuable data to study ACC behaviors. So far, in-depth analysis into more ACC behaviors using this rich dataset is not yet available.

Clearly, the current literature mainly focuses on the string stability of ACC from the control theory perspective or statistical difference between ACC and HDV behavior. A comprehensive in-depth analysis of the ACC behavior from the traffic flow perspective is missing. The aim of this paper is to understand how ACC behaves in different conditions (with respect to different ACC settings, traffic conditions, and stimulus) and the underlying impact mechanisms. The ultimate goal is to extrapolate the behavior of the general ACC systems and predict the impacts on traffic flow. To serve this goal, we have carefully designed a set of experiments with the inspiration from Gunter et al. (2020a) and Gunter et al. (2020b). We have tested three different car models, which will serve as our foundation for later extrapolation. Limited by scope, this paper only presents the results from one car model, referred to as Car Model X, but the analysis has been applied to the other two and will be presented in sequel papers.

Based on our experiments with Car Model X, we have obtained the following findings for a single ACC: (i) the ACC response time is comparable to human but much larger than the ACC controller time gap and it exhibits small variance,

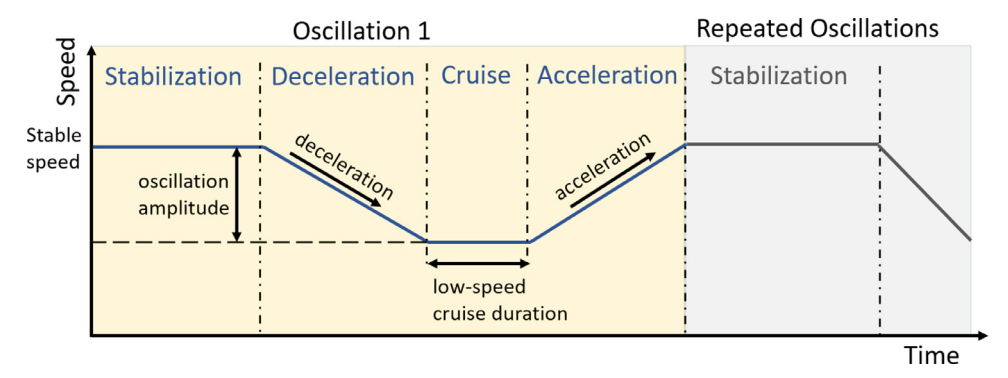


Fig. 1. Designed oscillation speed profile for the lead human-driven vehicle.

(ii) the ACC response can amplify or dampen an oscillation, (iii) after the oscillation, the stabilization process can exhibit overshooting or undershooting, and (iv) these behaviors depend largely on the ACC headway setting, speed level, and leader stimulus, where the impacts are produced directly and/or indirectly through the mediation of earlier ACC behaviors. For a three-vehicle platoon, our main finding is that the behavior change from one ACC vehicle to the next is progressive for oscillation growth, and regressive for deceleration, acceleration, and overshooting. This implies that in long platoons, oscillation amplitude tends to exacerbate very quickly, which forces ACC vehicles further upstream to apply very strong braking followed by a strong acceleration. This can cause significant overshooting and safety hazards.

The remainder of the paper is organized as follows: Section 2 introduces the experiment setup, Section 3 describes the methodologies to quantify the ACC behaviors, Section 4 presents the observations and mechanism of single ACC behaviors. Section 5 demonstrates the platoon effects. Section 6 provides discussions. Section 7 presents the conclusions.

2. Experiment setup

Our experiments use a three-vehicle platoon, where the lead vehicle is a human-driven vehicle followed by two identical ACC vehicles, namely ACC1 and ACC2. A high-accuracy GPS device uBlox EVK-M8T was installed on-board at the same position of each car (upper right of the windshield) to collect the location and velocity data at the resolution of 10 Hz. The average location and velocity error¹ of the GPS device are respectively around 0.89 m and 0.10 m/s, consistent with the scale reported in Gunter et al. (2020a).

During the experiment, the lead driver was instructed to produce a set of profiles that reflect different traffic conditions and stimulus. Fig. 1 shows a typical driving cycle, where the lead driver first traveled at a stable speed for an extensive period to ensure that it was in a stable state (set to be 30 s when the speed is < 45 mph (20.1 m/s), and 45 s for higher speed), then decelerated to a minimum speed, followed by cruising at the minimum speed for a period, and finally accelerated to resume the initial stable speed. Consecutive driving cycles were separated by a stable period to ensure that they start from a stable speed. The lead driver used cruise control to maintain the stable speed before the deceleration, during the low-speed cruise, and after acceleration, but the deceleration and acceleration were conducted manually. The speed profile was designed to mimic the traffic oscillations commonly seen in congested and/or near-saturated traffic in the real world (e.g., Chen et al., 2012; Tian et al., 2019). Note that Sharma et al. (2019) have identified six critical regimes (i.e., acceleration, deceleration, following, free acceleration, cruising without a leader, standstill) for general CF model calibration. In this paper, we focus on three of them that correspond to the constrained conditions, i.e., acceleration, deceleration, and following regimes.

To test the ACC behaviors, we have considered three categories of potential influential factors: (i) ACC headway - a feature of ACC controller, (ii) traffic speed level, and (iii) stimulus from the leader. For ACC headway, two levels were considered, small (headway-1) and large (headway-3) (headway is only shown on a relative scale on the dashboard and the specific values are unknown). Note that headway-3 is a medium (not the maximum) level headway setting on the tested vehicle (setting range: 1–7). The maximum headway setting was not used for the experiments because we found that in such a setting other road users frequently cut in and it was difficult to complete a driving cycle. Category (ii), called stable speed (speed level hereafter), referred to the travel speed before an oscillation starts and after the oscillation ends, in three levels (high, medium, and low). Category (iii) consisted of three components in a driving cycle, (1) oscillation amplitude: the speed reduction magnitude, in two levels (mild and strong), (2) low-speed cruise pattern: the duration of low speed in a driving cycle, in two levels (short - called dip, and long duration - called long-cruise) and (3) deceleration and acceleration maneuvers: the harshness of speed change, in two levels (mild and strong). Note that the three variables of category (iii) capture the strength of stimulus from different ways. The potential scenarios tested for each factor are shown in Table 1.

¹ We obtain the device error range by setting up two devices (with their antennas side by side) on one car and drive on the highway for about one hour. The error distribution is then produced by the speed/location differences between the data collected from the two devices.

Table 1Tested oscillation scenarios

Influential factor	Scenarios
Headway setting	a. Small : headway-1
	b. Large: headway-3
Stable speed	a. High: 65 mph (29.1 m/s)
	b. Medium: 45 mph (20.1 m/s)
	c. Low: 35 mph (15.6 m/s)
Oscillation amplitude	a. Small: 5 mph (2.2 m/s)
	b. Large: 10 mph (4.5 m/s)
Low speed cruise pattern	a. Dip: acceleration immediately
	b. Long-cruise: cruise for 10 s-15 s
Deceleration and acceleration maneuvers	a. Mild [†]
	b. Strong

[†]mild deceleration is always coupled with mild acceleration, same for the strong ones.

There are $2 \times 3 \times 2 \times 2 \times 2 = 48$ combinations of potential scenarios. We repeated twice for each combination, resulting in a total of 96 driving cycles for a car model.

The experiment was conducted on a public highway (for median/high speed) and a rural road (for low speed) with light traffic in a single day (sunny and dry). The road segments for the active runs have small slopes (max slope is 3%) and very mild curvature. The three tested vehicles always stayed in one lane. If other vehicles cut in, the data were discarded and we started a new cycle.

The same driver drove the lead HDV for the whole experiment. It is found the lead human driver has produced the designed speed profiles very well. The only exception is that there are variations in the executed deceleration and acceleration rates, which spread in a range rather than the discrete mild/strong setting. For that reason, our analysis will treat them as continuous variables. The two ACC vehicles were instructed to keep the ACC system activated throughout the experiment. The ACC desired speed was set higher than the leader stable speed to ensure the car-following mode. Both ACC1 and ACC2 were identical² mid-size electric car model with full speed range ACC function. The car model is commonly available on the market.

3. Methodology

This section presents the methods to process the data and measurements to quantify vehicle behaviors for the following analysis.

3.1. Data processing

In the raw GPS data, we have observed occasional noises. To handle them, we apply a de-noise process to the raw data. We first process the speed data to ensure the acceleration/deceleration kinematic is reasonable. Specifically, we apply a threshold of $(-5 \text{ m/s}^2 \text{ to } 4 \text{ m/s}^2)$ to the instantaneous acceleration/deceleration values derived from the speed data. Points outside the range are considered as irregular noises and replaced using the interpolation of the points before and after. We then apply a similar procedure on the location data, which should generate speed consistent with the direct speed measurement as the latter is accurate in general. Specifically, we apply a threshold of $(\pm 5 \text{ m/s})$ to the speed values derived from the location data. If the difference between the derived and measured speed is outside the range, the points are considered noisy and replaced using the interpolation of the points before and after.

After the de-noising process, we apply a small moving average window, 0.5 s, to the speed and location data. The main purpose is to make it easier to identify stable oscillation cycles (to present next). We have tested different moving average windows (from 0 s to 1 s) and found that the analysis outcomes are generally consistent.

3.2. Identification of critical maneuver time stamps

Fig. 2 illustrates the speed profile in a typical driving cycle after the data processing. Based on the leader's profile, we identify five critical time stamps within a cycle: the deceleration start time (T_{Ds}^L) and end time (T_{De}^L) , the acceleration start time (T_{As}^L) and end time (T_{Ae}^L) , and the minimum speed time $(T_{u_{min}}^L)$. Similarly, the five critical times for the follower are identified. Here, the subscripts denote the maneuvers. The superscripts differentiate the leading vehicle (L) and the following vehicle (F). The speed at the corresponding time is denoted by v (e.g., v_{Ds}^L is the speed of the leader at the deceleration start time).

² The two tested vehicles were manufactured in different years (ACC1: 2019, ACC2: 2018), but their ACC equipment is the same generation.

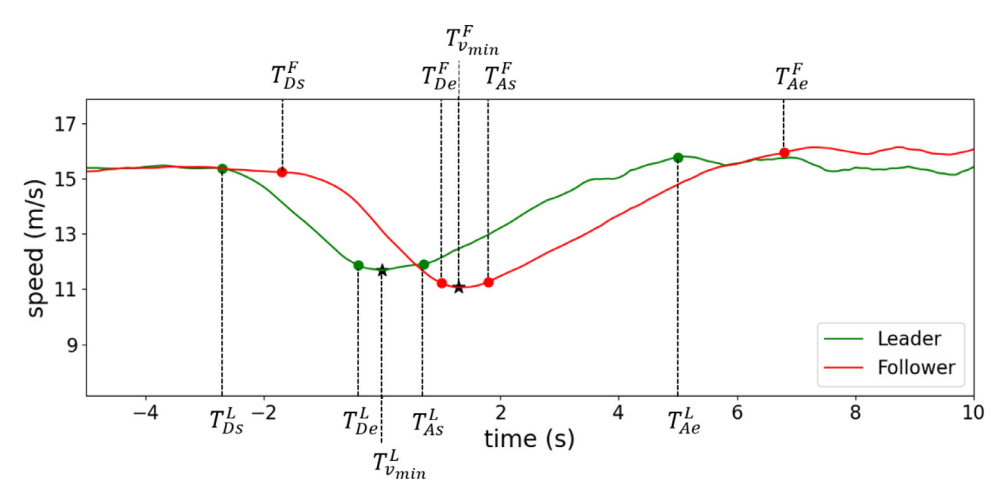


Fig. 2. Illustration of critical maneuver times (setting: Headway setting - Small, Oscillation amplitude - Strong, Cruise pattern - Dip, Deceleration and acceleration magnitude- Strong).

For the identification of the critical maneuver time stamps, the minimum speed $(T_{\nu_{\min}})$ is directly identified by the lowest speed in the oscillation cycle. We then use the wavelet transform algorithm per Zheng et al. (2011) to identify the deceleration start (T_{Ds}) and acceleration end time (T_{Ae}) , as they are characterized with significant speed changes (see Appendix A for the details of wavelet transform application).

For the deceleration end time (T_{De}) and acceleration start time (T_{As}) , they do not have significant speed changes. Thus, we identify them via two thresholds. T_{De} is recognized in the period before $T_{\nu_{\min}}$ as the furthest point that satisfies both (i) speed threshold - the speed deviation from the minimum speed (ν_{\min}) is within 0.5 mph (0.22 m/s), and (ii) acceleration/deceleration rate threshold - the deceleration/acceleration rate is within 1/3 of the maximum rate (absolute value). T_{As} is identified in the similar way but in the period after $T_{\nu_{\min}}$. These two thresholds together ensure that during (T_{De}, T_{As}) , the vehicle is adjusting its speed around ν_{\min} with very small speed change. Several other values are tested for the two thresholds (0.22 m/s, 0.34 m/s, and 0.45 m/s for the speed threshold and 1/5, 1/4, 1/3 for the rate threshold) and they show similar results.

3.3. Selection of stable oscillation cycles

Another important step in data processing is to ensure a driving cycle starts from a steady state so that it is not affected by previous residual disturbances. For this purpose, we consider 10s before the deceleration start time (T_{Ds}^L) and apply two thresholds, requiring that during the 10s period, (i) the spacing between the leader and follower has a variation ≤ 2 m, and (ii) the maximum speed difference between the leader and follower does not exceed 0.89 m/s (2 mph). Other values (1 m for spacing and 0.45 m/s for speed difference) have been tested and the results of the overall analysis are similar.

3.4. ACC behavior variables

For the car-following (CF) behaviors of the ACC vehicle, we consider three main aspects, response time, deceleration and acceleration process, and speed evolution during the oscillation. To quantify them, several behavior variables are defined and measured from the data; see Table 2 for the definition of the variables.

The response time (ΔT) is defined as the difference of the deceleration start time between the ACC and leader. This is the detectable time lag that one would observe (different from the controller time gap), similar to the definition per Makridis et al. (2019b). The average deceleration rate (d_{avg}) and acceleration rate (a_{avg}) measures the average speed change rate during the deceleration (acceleration) process. Note that we take the absolute values of these rates. Furthermore, we obtain the ACC deceleration (acceleration) rate change compared to the leader, denoted as Δd_{avg} and Δa_{avg} .

The speed evolution across vehicles in the platoon during oscillations is highly related to the stability and efficiency (Chen et al., 2012) (e.g., whether an oscillation is amplified or dampened). The oscillation amplitude (Ω) is calculated by the difference between stable speed and minimum speed (v_{Ds} v_{min}). The oscillation growth (ϕ) measures the change of oscillation amplitude compared to the leader, defined as the minimum speed differences between the follower and leader (the value is equal to Ω^F Ω^L , since $v_{Ds}^F = v_{Ds}^F$). It captures the extra speed reduction by the follower, and directly reveals the

³ In our data, the deceleration/acceleration rate is mostly $\leq 1.5 \text{ m/s}^2$ and thus this threshold is stricter than the 0.05g in the literature (Ozaki, 1993; Ali et al., 2018)

Table 2Behavior variable list .

Notation	Variable	Definition
ΔT d_{avg} a_{avg} Δd_{avg} Δd_{avg} Δa_{avg} Δa_{avg}	Response time Average deceleration rate† Average acceleration rate† Change of average deceleration rate Change of average acceleration rate Oscillation amplitude	$\begin{array}{l} \Delta T = T_{Ds}^F T_{Ds}^L \\ d_{avg} = (v_{Ds} \ v_{De}) \ / \ (T_{Ae} \ T_{As}) \\ a_{avg} = (v_{Ae} \ v_{As}) \ / \ (T_{De} \ T_{Ds}) \\ \Delta d_{avg} = a_{avg}^F \ d_{avg}^A \ d_{avg}^A \\ \Delta a_{avg} = a_{avg}^F \ a_{avg}^A \end{array}$
$\phi \ \psi$	Oscillation growth Overshooting	$\phi = v_{min}^L \ v_{min}^F \ v_{min}^E \ \psi = v_{Ae}^F \ v_{Ae}^L$

 $^{^{\}dagger}$ In our analysis, we have also used maximum deceleration/acceleration rates and the results are found to be similar with the average rates.

string stability of the ACC controller (Gunter et al., 2020a). The overshooting effect (ψ) is defined as the speed difference between the leader and follower at the acceleration end time.

3.5. Asymmetric behavior (AB) framework

We adopt the asymmetric behavior CF framework (Chen et al., 2012) to help explain the car-following mechanism of ACC. The AB model is an extension of Newell's simplified car-following model (Newell, 2002), which gives the exact numerical solution of the kinematic wave model (Lighthill and Whitham, 1955; Richards, 1956) with triangular fundamental diagram. In congestion, Newell's model predicts that the trajectory of a follower is identical to that of its leader except for a translation in space-time; we call this trajectory "Newell trajectory", which represents the average/equilibrium behavior in our context. Specifically, η is the indicator in the model that describes the deviation of the driver with respect to the Newell trajectory. If η < 1 then the vehicle is in front of the Newell trajectory and therefore driving more aggressively than the average; similarly, η > 1 implies a more timid driving behavior.

In this paper, we calculate η using the following equation:

$$\eta(t) = \frac{x_{i-1}(t - \tau_0) - x_i(t)}{\delta_0},\tag{1}$$

where τ_0 , δ_0 are the time shift and space shift in the Newell trajectory, which is equivalent to the time gap at equilibrium and the jam spacing, respectively. The $x_i(t)$ denotes the location of vehicle i at time t, and vehicle i-1 is the leader of vehicle i. This measured η indicates the spacing deviation of the vehicle from the equilibrium. τ_0 and δ_0 are estimated from the collected empirical data and treated as constants under the same headway setting. Specifically, we acquire the equilibrium periods (where the spacing and speed are both stable) from the trajectory data, and then estimate the two parameters from a linear spacing-speed relationship, in which τ_0 is the slope and δ_0 is the intercept. Based on the estimation results, in headway-1, $\tau_0 = 0.49$ s, $\delta_0 = 16.88$ m. In headway-3, $\tau_0 = 0.84$ s, $\delta_0 = 16.31$ m. The values are consistent with the scale reported in other field tests (Gunter et al., 2020a).

4. Single ACC dynamics

In this section, we focus on the behaviors of the first ACC vehicle in the platoon, ACC1, to study the single ACC CF dynamics. The behavior of the 2nd ACC, ACC2, will be analyzed in the next section. In total, 93 stable oscillation cases were collected, with 46 dip and 47 long-cruise cases. These two types have some unique features and will be presented separately.

Note that, in the experiment, the three categories of influential factors defined in Section 2 are our independent variables (IVs). For the ACC response, we focus on five sequential ACC behavior features throughout an oscillation cycle, response time (ΔT), deceleration rate change (Δd_{avg}), oscillation growth (ϕ), acceleration rate change (Δa_{avg}), and overshooting (ψ). Namely, these five variables are our dependent variables (DVs). We are interested in the relationship between the IVs and the DVs and the impact mechanisms.

4.1. Dip cases

For the analysis of ΔT and Δd_{avg} , all 93 sample cases are used as these are features of ACC in the deceleration process shared by both dip and long-cruise cases. For the other three components, only the 46 dip cases are used as they are features involving ACC acceleration. In Section 4.1.1 we will first characterize the five ACC behavior features by their sequential order and then analyze the underlying mechanisms in Section 4.1.2.

4.1.1. ACC Behavior features Response time ΔT

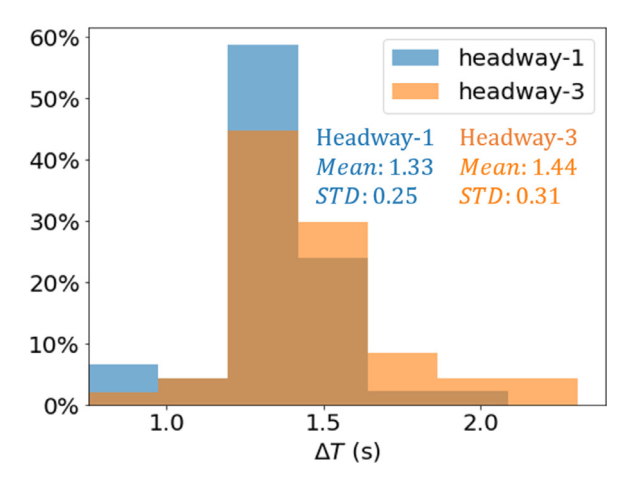


Fig. 3. Distribution of ΔT in ACC1.

Table 3 Multiple linear regression results on ΔT (model R^2 : 0.204, sample size: 93).

IV	Impact coefficient	
Headway	0.112*	
Speed	0.011*	
d_{avg}^L	0.241*	

^{*}indicate significantly different from zero at 95% confidence level.

 ΔT captures how responsive the ACC is upon detecting the leader's deceleration. Fig. 3 shows the distribution of ΔT in headway-1 and headway-3. The observed ΔT is comparable to human drivers and the ACC systems tested in other experiments (Makridis et al., 2019a; 2019b). Notably, ΔT is much larger than the time-gap of the ACC controller, τ_0 . The mean of ΔT is 1.33 s for headway-1 and 1.44 s for headway-3, compared to $\tau_0 = 0.49$ s and $\tau_0 = 0.84$ s, respectively. This suggests that the ACC vehicle is in non-equilibrium during the oscillation cycles.

Remark R1: The response time ΔT is much larger than equilibrium time gap and is not totally stochastic. Instead, ΔT is positively impacted by headway and speed, and negatively impacted by leader deceleration rate d_{avg}^L . The results are shown in Table 3.

We obtain the results above by doing multilinear regression on ΔT using the three potential IVs. In the regression, headway is set as a discrete variable (0: headway-1, 1: headway-3) and the other two variables are continuous variables.

The three IVs together can explain 20.4% of the variance observed in ΔT . The prediction capability of the fitting is not very high. This may be because the relationship is not linear or there is significant randomness.

Deceleration rate change Δd_{avg}

Once the ACC starts the response to the leader, Δd_{avg} reflects how strong the ACC vehicle decelerates compared to the leader's deceleration, i.e., positive means stronger deceleration, and thus an aggressive response, and negative means the opposite.

Fig. 4 shows the mean and 10% and 90% percentile of Δd_{avg} at different headway and speed. One can see that Δd_{avg} is mostly positive for headway-1 (red plot) but negative for headway-3 (green plot), suggesting that ACC responds aggressively under small headway but gently under large headway. Additionally, Δd_{avg} varies in a large range. Moreover, while the mean of Δd_{avg} is small, it differs from zero significantly in some headway and speed combinations (i.e., low speed in headway-1 and medium/high speed in headway-3). This suggests that the deceleration rate change can escalate quickly in a long platoon and produce a profound effect (We will look into the platoon effect in Section 5).

Now we want to further investigate the impacts of the IVs on Δd_{avg} . Note that now we have two dependent variables, and ΔT occurs beforehand. Therefore, the IVs can impact Δd_{avg} directly and/or indirectly via ΔT . To investigate such a relationship, we use the mediation analysis (Hayes, 2017), which is widely used in many disciplines (Alter and Balcetis, 2011; Costa and Pinto-Gouveia, 2011; Ruby et al., 2011).

The mediation test is used to quantify the direct and indirect effects among the independent variable X, dependent variable Y, and the mediator M, as shown in Fig. 5. The test involves three steps, where step 1 regresses Y on X, step 2 regresses M on X, and step 3 regresses Y on X and M; see (2)–(4). Here, the coefficients c quantifies the strength of the total effect of X on Y, which consists of two parts, c' for the direct effect from X, and (a*b) for the indirect effect (equals to c-c'). The signs indicate the correlation direction: + for positive and for negative. The significance of the mediation effect is equivalent to the significance of the corresponding coefficient. More specifically, the significance of direct and total effect

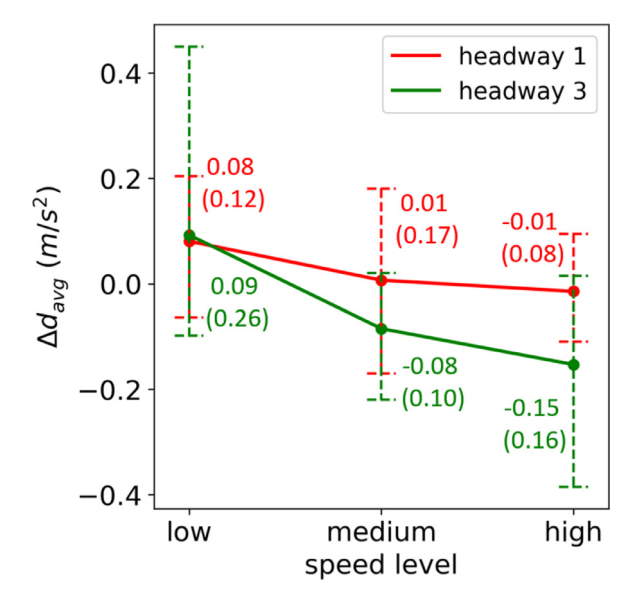


Fig. 4. Deceleration rate change Δd_{avg} in ACC1.

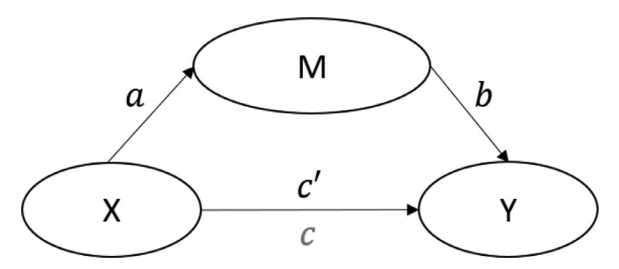


Fig. 5. Sketch of mediation analysis.

Table 4 Mediation analysis results on Δd_{avg} (mediator: ΔT , total fitting R^2 : 0.478, sample size: 93).

		Impact coefficient	
IV	Indirect	Direct	Total
Headway	0.037*	0.114*	0.077*
Speed	0.004*	0.017*	0.014*
d_{avg}^L	-0.080*	0.053	0.133*

^{*} Significance at 95% confidence level and no start indicates insignificance.

is revealed by the p-value in the linear regression process. The significance of the indirect effect is determined using the bootstrapping approach (Preacher and Hayes, 2004), which uses a re-sampling procedure to estimate the variance of the indirect effect and produces the upper and lower bounds for a given confidence level. If the confidence interval (from lower to upper bound) of coefficient (a*b) does not cover zero, it is significant and otherwise insignificant.

$$Y = i_0 + cX + e_1 \tag{2}$$

$$M = i_1 + aX + e_2 \tag{3}$$

$$Y = i_2 + c'X + bM + e_3 (4)$$

For Δd_{avg} , ΔT is a potential mediator. Table 4 summarizes the mediation analysis outcome. Note that we have three independent IVs. They are all used in the regressions, and when we investigate the mediation effect of one IV, the other IVs are covariates (i.e., they are controlled). The mediation analysis is conducted with the R package 'PROCESS'. We omit the detailed analysis process for brevity but the audience is referred to Hayes (2017).

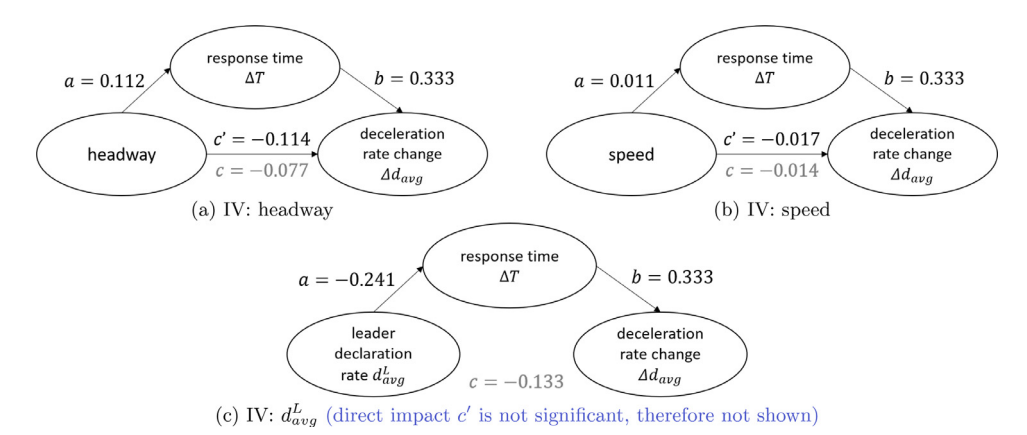


Fig. 6. Impacts of headway, speed, and d_{avg}^L on Δd_{avg} (mediator: ΔT , total fitting R^2 : 0.478) .

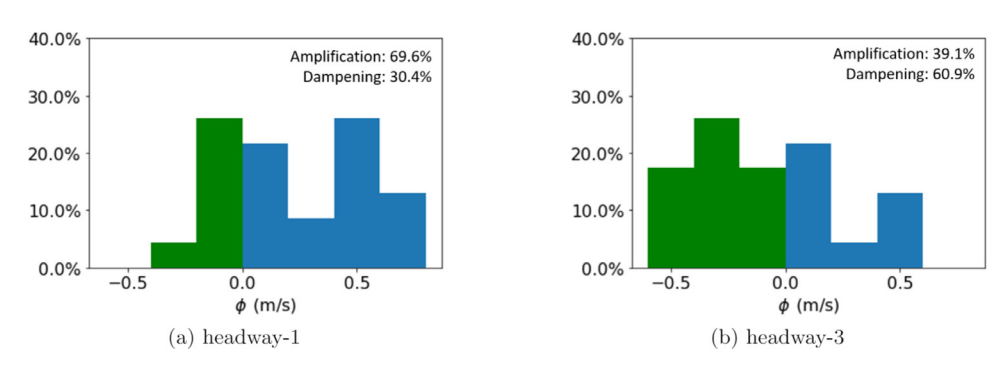


Fig. 7. Distribution of oscillation growth ϕ in ACC1.

Fig. 6 shows how each IV impacts Δd_{avg} using the statistical diagram (Hayes, 2017). For headway (see Fig. 6(a)), one can see that it has a negative direct effect and a positive indirect effect mediating through ΔT . For the indirect effect, it means that the increase of headway will result in the increase of ΔT , which in turn increases Δd_{avg} because of the influence of ΔT on Δd_{avg} , i.e., larger headway indirectly leads to larger Δd_{avg} . The direct and indirect effects here have different signs, suggesting that the direct effect of headway on Δd_{avg} is suppressed by the mediation through ΔT . However, the direct effect dominates and thus the total effect remains negative. Speed impacts Δd_{avg} in a similar fashion; see Fig. 6(b). For d_{avg}^L , interestingly, its direct effect is insignificant but the indirect effect is significant, suggesting that its impact is fully mediating through ΔT ; see Fig. 6(c).

Remark R2: regarding Δd_{avg} , headway, speed, and d_{avg}^L all have a negative total effect, and they all have an indirect effect mediating through ΔT .

Oscillation growth ϕ

In the end of the deceleration process, ϕ captures the evolution of oscillation amplitude as it passes from the leader to the follower. This feature is an indicator of the string stability of the ACC behavior (Naus et al., 2010b; 2010a). A positive ϕ suggests that the follower amplifies the oscillation and thus it is not string stable. Otherwise, it is a dampening effect and it is string stable.

We observe that ϕ is mostly positive for the smaller headway but is more likely negative for the larger headway; see Fig. 7 (blue bins denote amplification with $\phi \geq 0$; green bins denote dampening with $\phi < 0$). The value of ϕ is profound in many cases, implying that the oscillation amplitude will change significantly as it propagates against traffic. Particularly, the amplification is profound at low speed in headway-1 (mean is 0.43 m/s) while dampening is profound at high speed in headway-3 (mean is 0.39 m/s), suggesting that oscillation can exacerbate or smooth out quickly in a platoon (Fig. 8).

To further study the impacts of IVs on ϕ , we do the similar analysis as for Δd_{avg} . Note that now we have two potential serial mediators, ΔT and Δd_{avg} , in which ΔT influences Δd_{avg} . We follow the procedure per Hayes (2017) to conduct the analysis.

Remark R3: regarding ϕ , (i) both amplification and dampening are observed; (ii) headway has a total negative effect on ϕ and the effect is partially mediating through ΔT and Δd_{avg} ; (iii) speed has a total negative effect on ϕ and the effect is partially mediating through Δd_{avg} ; and (iv) d_{avg}^L has a total positive effect on ϕ , and the indirect effect is negligible.

Table 5 summarizes the results and Fig. 9 shows the detailed relationships. The impacts of IVs on ϕ are complicated now as two serial mediators are involved. For headway (see Fig. 9(a)), it impacts ϕ both directly and indirectly. Particularly, it

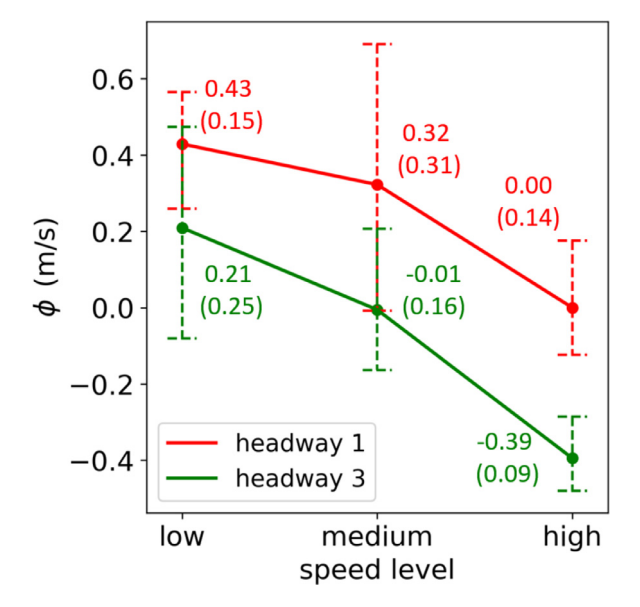


Fig. 8. Oscillation growth ϕ in ACC1.

Table 5 Mediation analysis results on ϕ (mediators: ΔT and Δd_{avg} , total fitting R^2 : 0.844, sample size: 46).

	Impact coefficie	ent	
IV	Indirect	Direct	Total
Headway	0.100*	0.212*	0.312*
Speed	0.019*	0.016*	0.035*
d_{avg}^L	0.028	0.298*	0.270*

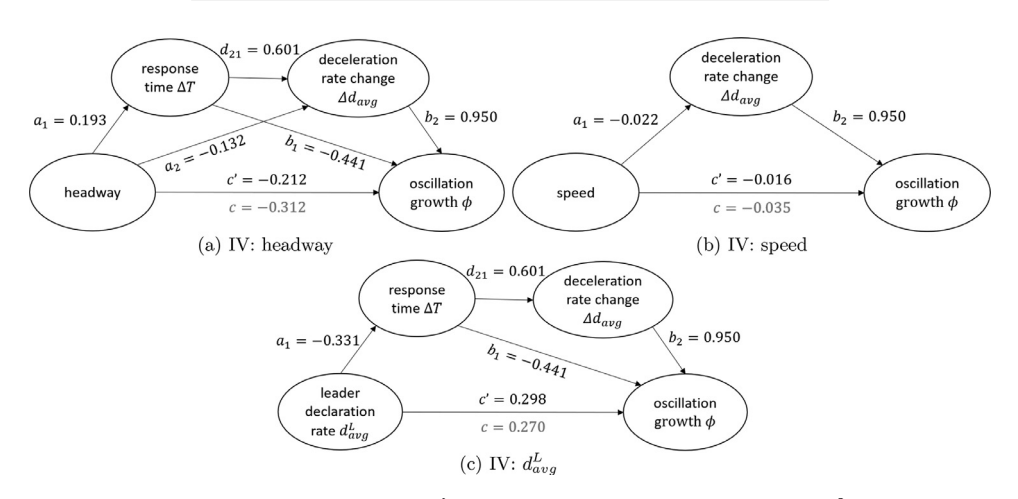


Fig. 9. Impacts of headway, speed, and d_{avg}^{L} on ϕ (mediator: ΔT and Δd_{avg} , total fitting R^2 : 0.844).

has a direct negative effect. On the indirect effect, there are three indirect paths, headway $\to \Delta T \to \phi$, headway $\to \Delta d_{avg} \to \phi$, and headway $\to \Delta T \to \Delta d_{avg} \to \phi$. Compared to R2, three new correlations are observed: (i) headway has a negative influence on ϕ , (ii) ΔT has a negative influence on ϕ , and (iii) Δd_{avg} has a positive influence on ϕ . The three indirect paths have similar strength but one has an opposite sign. Nevertheless, the total indirect effect is negative, aligned with the direct effect. Moreover, the direct effect is much stronger.

For speed (see Fig. 9(b)), it only mediates through Δd_{avg} (the mediation through ΔT is insignificant). The direct and indirect effects are both negative and with similar strength. For d_{avg}^L (see Fig. 9(c)), two indirect paths are significant but they counter each other, resulting in a negligible total indirect effect. The positive direct effect dominates. This result implies that the strength of stimulus (represented by d_{avg}^L) affects the ACC stability.

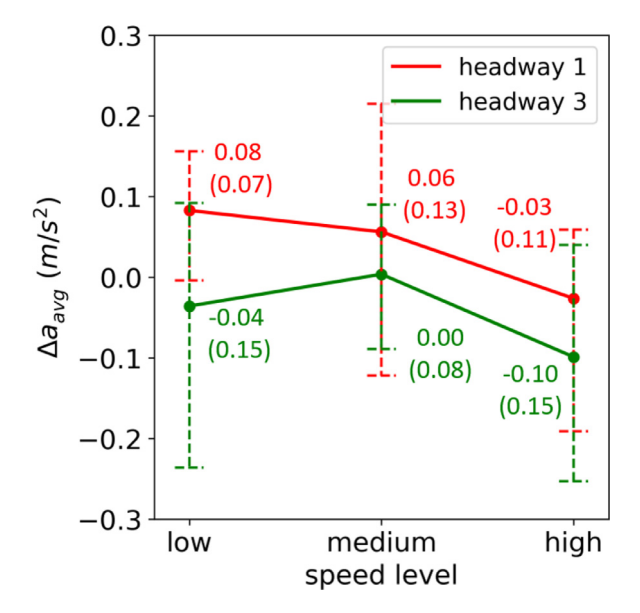


Fig. 10. Acceleration rate change Δa_{avg} in ACC1.

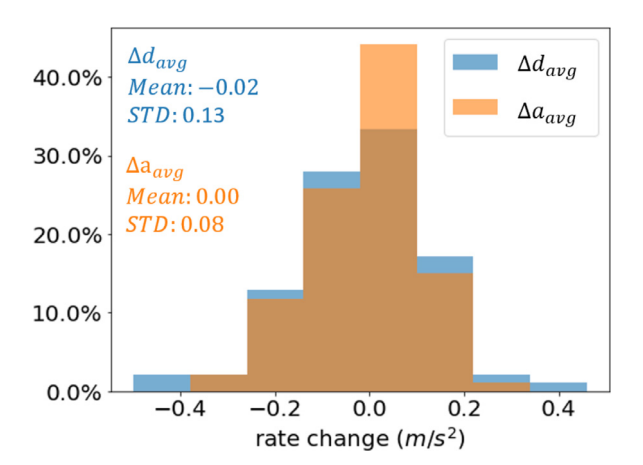


Fig. 11. Distribution of ACC deceleration and acceleration rate change.

Note that, another IV, oscillation amplitude Ω , can potentially impact ϕ too. However, the data of Ω and d_{avg}^L are correlated because of the limitation in our experiment execution. Such correlation can result in an unreliable outcome of the significance (Graham, 2003). Therefore, in our regression analysis, only one of them is used. We repeat the same analysis using only Ω and find that the model performances are similar (i.e., R^2 scores are similar and the signs of various effects from headway and speed are the same). This is not surprising as these two both capture the strength of stimulus, though from different perspectives. It is possible that Ω and/or d_{avg}^L will effect ϕ . Further research is needed to isolate their effects. Acceleration rate change Δa_{avg}

In the acceleration process, Δa_{avg} reflects how strong the ACC vehicle accelerates compared to the leader's acceleration, i.e., positive means stronger acceleration and thus more aggressive response and negative means the opposite.

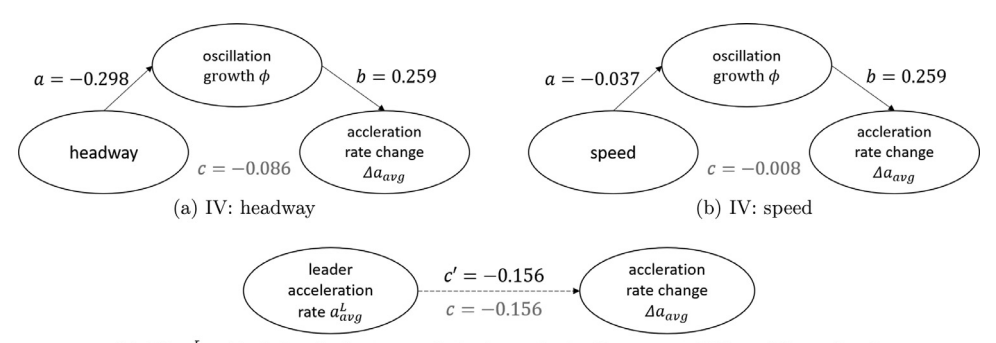
From Fig. 10, one can see that Δa_{avg} has a large variation and the mean is only significantly different from zero at low speed in headway-1. For other speed and headway combinations, the mean is insignificant from zero, which may be due to the large variation. Nevertheless, Δa_{avg} can still be quite significant in many cases (50% cases in headway-1 low/medium speed has a rate change larger than 0.05 m/s², and 38% cases at headway-3 high speed level has rate change smaller than -0.05 m/s^2). Similar to the deceleration rate change, such an impact will escalate in a platoon as we will see later. It is also interesting to note that, compared to Δd_{avg} , Δa_{avg} varies in a smaller range (in both sides) and concentrate more on small values (Fig. 11).

We conduct the same mediation analysis to investigate the impacts of IVs on Δa_{avg} . Note that three potential mediators can exist, ΔT , Δd_{avg} , and ϕ , as they all occur prior to the acceleration. However, our analysis using the three mediators found that the mediation paths involving ΔT and/or Δd_{avg} have insignificant effects. Thus, we only keep ϕ as the mediator.

Table 6 Mediation analysis results on Δa_{avg} (mediators: ϕ , total fitting R^2 : 0.356, sample size: 46).

	Impact coefficie	ent	
IV	Indirect	Direct	Total
Headway	0.077*	0.009	0.086*
Speed	0.010*	0.002	0.008*
a_{avg}^L	-	0.156+	0.156+

- * that indicates a 95% significance level.
- ⁺ indicate significantly different from zero at 90% confidence level.



(c) IV: a_{avg}^L (dash line indicates a relatively weak significance, at 90% confidence level)

Fig. 12. Impacts of headway, speed, and a_{avg}^L on Δa_{avg} (mediator: ϕ , total fitting R^2 : 0.356).

Remark R4: regarding Δa_{avg} , (i) headway has a total negative effect on Δa_{avg} and the effect is fully mediating through ϕ ; (ii) speed impacts Δa_{avg} in a similar way as headway; and (iii) leader acceleration rate (a_{avg}^L) has a direct negative effect on Δa_{avg} .

Table 6 summarizes the results and Fig. 12 shows the detailed relationships. The effects from headway and speed are both fully mediating through ϕ ; i.e., the direct effects are insignificant. Specifically, the mediator, ϕ , has a positive influence on Δa_{avg} . The result suggests that an increase of headway (or speed) will result in a decrease in ϕ , which in turn causes a decrease in Δa_{avg} . For the a_{avg}^L , it does not affect the mediator (oscillation growth occurs prior to acceleration) and produces a negative direct effect though the significance is slightly weak (at 90% confidence level).

Note that our analysis above used a_{avg}^L as an IV. Potentially, d_{avg}^L and Ω can impact Δa_{avg} too. However, our data of the three variables, a_{avg}^L , Ω , and d_{avg}^L , are correlated because of the limitation in our experiment execution. We have repeated the analysis by replacing a_{avg}^L with either d_{avg}^L or Ω , and found that the model performances are generally similar (i.e., similar R^2 score and the directions of impacts from speed and headway are similar). But when d_{avg}^L is used, its direct and indirect effects counter each other and the negative total effect is insignificant. When Ω is used, it has a positive total effect, but its direct and indirect effects are both insignificant. Nevertheless, the results suggest that the three variables describing stimulus strength in general have similar effects on Δa_{avg} . Moreover, the strength of the stimulus, either in d_{avg}^L , Ω , or a_{avg}^L , is possible to affect Δa_{avg} , but the impact mechanism is likely complex. Further research is needed to isolate and quantify the impact of each of the three variables.

Overshooting ψ

In the end of the acceleration process, the ACC vehicle has a stabilization process - to adjust its spacing with the leader and stabilize at the initial speed level like the leader. In this process, overshooting ψ describes how much the ACC speed exceeds the leader's speed. Note that overshooting is an important feature for controller design (e.g., Milanés and Shladover, 2014). Particularly, in the literature of controller testing (Ploeg et al., 2011; Milanés and Shladover, 2014), overshooting is often associated with oscillation amplification and thus it is also an indicator of string stability. It is worth noting that, the overshooting in the reported studies is usually dramatic - characterized by an obvious speed increase in a short period of time. However, in our data, the overshooting is much more gradual, i.e., the excessive speed is small but can last for a significant period; see Fig. 13. The 90 percentile of overshooting in our data is 0.57 m/s, which is much smaller than the value (about 1 m/s) in Milanés and Shladover (2014). Moreover, our tested ACC sometimes displays an undershooting behavior (i.e., negative overshooting) - the ACC vehicle uses a speed smaller than the leader throughout the stabilization process. Similar to overshooting, the undershooting observed is also characterized by a gradual process with a small magnitude of speed difference. Such a characteristic of overshooting/undershooting process can be clearly observed in the empirical example later illustrated in Fig. 16.

Regarding the impacts of IVs on ψ , only ϕ is kept as the mediator as the others (ΔT , Δd_{avg} , Δa_{avg}) produce insignificant effects. Table 7 summarizes the results and Fig. 14 shows the detailed relationships. The mediator ϕ is found to have a

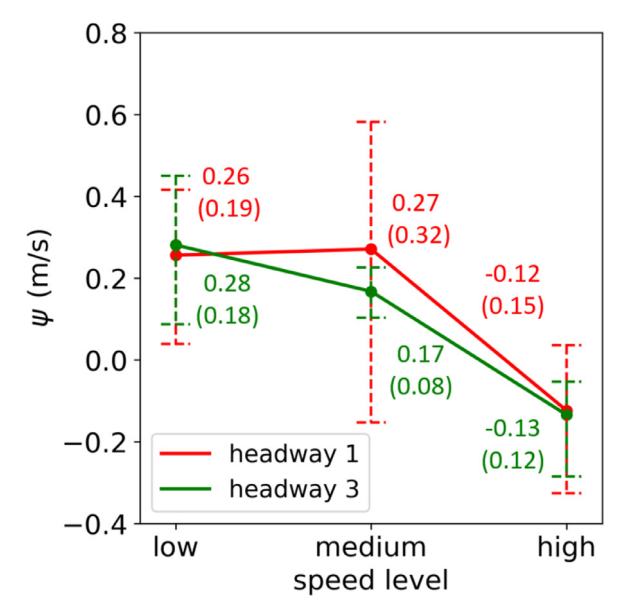


Fig. 13. Overshooting ψ in ACC1.

Table 7 Mediation analysis results on ψ (mediators: ϕ , total fitting R^2 : 0.639, sample size: 46).

	Impact coefficie	ent	
IV	Indirect	Direct	Total
Headway	0.197*	0.167*	0.030
Speed	0.023*	0.007	0.030*
Ω	0.073*	0.012	0.061*

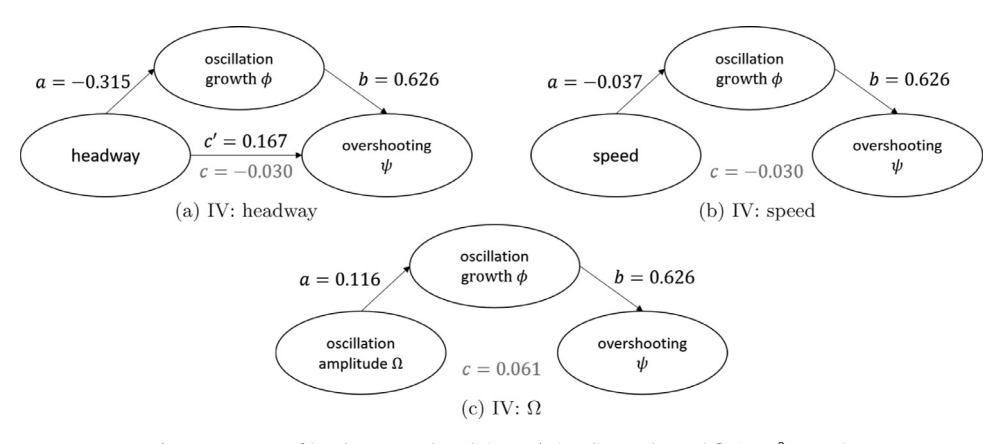


Fig. 14. Impacts of headway, speed, and Ω on ψ (mediator: ϕ , total fitting R^2 : 0.639).

positive influence on ψ , i.e., a larger ϕ leads to larger ψ . For headway, it has a negative indirect effect mediating through ϕ and a positive direct effect (see Fig. 14(a)), which cancels out and results in a negligible total effect. For speed, the negative effect is fully mediating through ϕ ; see Fig. 14(b). Similarly for Ω , the positive effect is fully mediating through ϕ ; see Fig. 14(c).

In the analysis above, again, either d_{avg}^L or a_{avg}^L can potentially impact overshooting too. We have repeated the analysis by replacing the third IV with d_{avg}^L or a_{avg}^L and found the model performances are generally similar. When d_{avg}^L is used, it produces a positive effect fully mediating through growth, similar to the case using Ω . When a_{avg}^L is used, it has a dominant

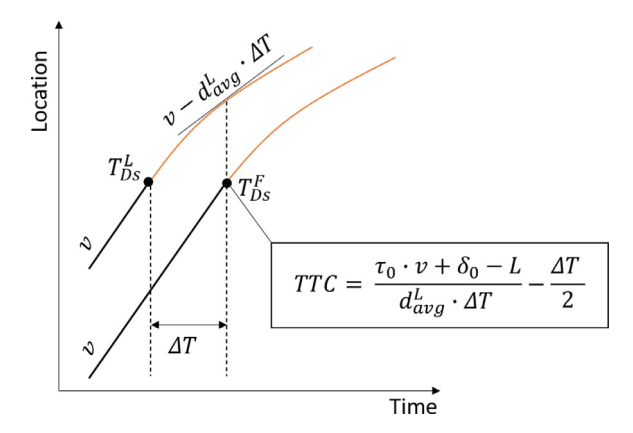


Fig. 15. Impact of speed, headway, d_{avg}^L , and ΔT on safety risk (L - vehicle length).

positive direct effect and a negative indirect effect mediating through Δa_{avg} . A Nevertheless, either d_{avg}^{L} or a_{avg}^{L} has produced a total positive effect on Δa_{avg} , consistent with our result above using Ω .

Remark R5: regarding the overshooting effect, (i) both overshooting and undershooting are observed; (ii) headway has a negligible total effect on ψ ; (iii) speed has a negative effect on ψ fully mediating through ϕ ; and (iv) Ω has a direct positive effect on ψ fully mediating through ϕ .

4.1.2. Behavior mechanisms

This section aims to interpret the underlying mechanisms for the remarks on the ACC behaviors in the subsection above. Mechanism of response time ΔT

Per R1, ΔT is not totally stochastic, but positively correlated with headway and speed, and negatively correlated with d_{ayo}^L . This may seem unexpected. However, it is not uncommon to have a delay term in the design of quadratic controllers, such as Zhou and Ahn (2019). As for the correlation, it can be interpreted in this way: once the leader starts to decelerate, ACC has to decelerate to avoid a crash. Since ACC decelerates with a time lag, the safety risk increases in this process until the ACC deceleration starts. Particularly, the safety risk is larger if speed is smaller, headway is smaller, or d_{ayp}^L is larger. As a result, ACC compensates the larger risk by responding more promptly; i.e., ΔT is smaller. This potential mechanism is illustrated in Fig. 15. Consider the time-to-collision (TTC) value⁵ (Hayward, 1972), which reversely indicates safety risk (see the formulation in Fig. 15). Obviously, TTC at the follower deceleration start point decreases with d_{avg}^L but increases with speed and headway (indicated by τ_0). Also, TTC will increase if ΔT decreases, i.e., a smaller ΔT can compensate the adverse effect caused by d_{avg}^L , speed and headway.

Mechanism of deceleration rate change Δd_{avg} Per R2, the indirect effect indicates ΔT has a positive influence on Δd_{avg} . This is expected. With all other factors controlled, when ACC responds with a larger lag (i.e., a larger ΔT), TTC is smaller and safety risk is higher, which will in turn demand a stronger deceleration to ease the safety risk - with a larger Δd_{avg} , ACC can reduce the risk faster.

Regarding the direct effect, per R2, speed and headway have direct negative effects on Δd_{avg} , which suggests that, if everything else (like ΔT) is controlled, a smaller speed/headway will directly result in a larger Δd_{avg} . This is straightforward. Note that ΔT is much larger than τ_0 . Thus, when ACC starts to decelerate, its speed is larger than the leader and the spacing is below the equilibrium. At this time stamp, the safety risk negatively correlates with headway and speed (see the formulation of TTC). Therefore, with ΔT controlled, a smaller headway/speed implies larger safety risk and will directly call for a stronger Δd_{avg} to compensate the safety risk. Such an effect remains strong even after it is suppressed by the indirect effect. Accordingly, we see a significant negative total effect.

It is puzzling that d_{avg}^L does not show a similar significant direct effect on Δd_{avg} , though ACC should also have a higher risk when d_{avg}^L is larger when it starts deceleration. We conjecture that there is another mechanism impacting Δd_{avg} through d_{avg}^{L} . Recall that Δd_{avg} is the difference between the deceleration of ACC and the leader. One possibility is that, when the leader uses a stronger deceleration, the ACC controller does not respond as strongly because ACC has a constraint on comfort. As a result, the deceleration rate change, Δd_{avg} , becomes smaller. Future research is needed to test our conjecture.

Overall, R1 and R2 together suggest that, at a smaller speed or headway, while ACC responds more promptly to reduce the safety risk, a stronger Δd_{avg} is still needed to further compensate the risk. Fig. 16 provides four empirical cases. From Fig. 16(a) to (b), when headway setting increases from 1 to 3, ΔT increases from 1.4 s to 1.5 s. One can see that the ΔT increase is in a small scale. Along with that, Δd_{avg} decreases from 0.13 m/s² to -0.15 m/s², showing a total negative effect

 $^{^4}$ For this case, ϕ cannot be a mediator and Δa_{avg} turns out to be an active one.

⁵ TTC is defined as the time until a collision between would have occurred if the speed difference is maintained. Smaller TTC indicates larger risk.

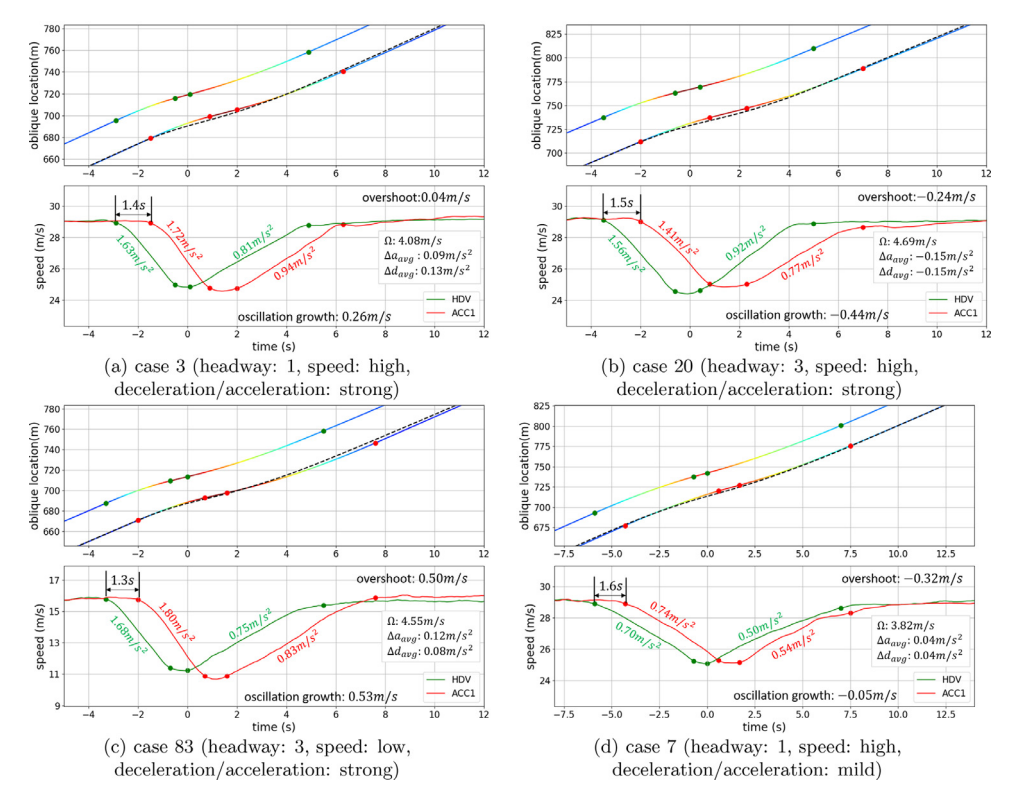


Fig. 16. Empirical cases.

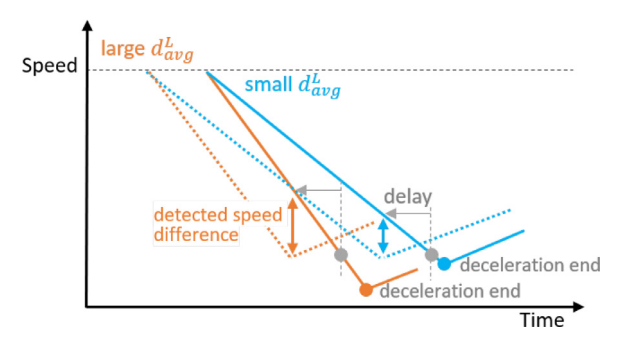


Fig. 17. ACC detected speed difference related to d_{avg}^L during deceleration (Δd_{avg} is assumed 0 for simplicity).

from headway. Meanwhile, (c)-(b) shows the impact of speed; i.e., when speed increases from 15.6 m/s in Fig (c) to 29.1 m/s in Fig.(b), ΔT increases from 1.3 s to 1.5 s, showing the positive effect on ΔT , and Δd_{avg} decreases from 0.08 m/s² to -0.15 m/s², showing the negative effect on Δd_{avg} . (d)-(a) shows the impact of d_{avg}^L ; i.e., when d_{avg}^L increases from 0.70 m/s² to 1.63 m/s², ΔT decreases from 1.6 s to 1.4 s, showing the negative effect (the impact of d_{avg}^L on Δd_{avg} is not significant in this specific case).

Mechanism of oscillation growth ϕ

Per R3-(ii), smaller headway *directly* results in larger ϕ . We conjecture that this is because different headways result in different desired spacings and that impact the controller sensitivity, or the controller has different parameters under different headways (e.g., more sensitive in smaller headway). Note that ϕ itself is a cumulative outcome of ACC behavior throughout the deceleration process. With the change in controller parameters, headway can affect the ACC behavior in every time stamp and that accumulates to oscillation growth. Per R3-(ii), smaller speed also *directly* leads to larger ϕ . We have a similar conjecture that speed (or its relevant term) is included in the state space of the controller, which is very common in controller design (Zhou and Ahn, 2019), and that produces a persistent effect that accumulates during the deceleration process and affects ϕ .

R3-(iv) indicates that larger d_{avg}^L leads to larger ϕ . This is likely related to the systematic delay of the controller. Fig. 17 shows a sketch for the mechanism. Consider two cases with a large d_{avg}^L (orange lines) and a small d_{avg}^L (blue lines). The

dash line is the leader and the solid line is the follower ACC. Here, all other behavior features (e.g., ΔT , Δd_{avg} , Ω) are controlled the same, and only d_{avg}^L differs. When ACC speed equals to the minimum speed of the leader (denoted by grey points), due to the delay ΔT (denoted by the gray arrow), it detects the speed difference at ΔT earlier (at the vertical arrow point), which yields a larger speed difference if d_{avg}^L is larger, see the orange arrow vs. the blue one. With a larger speed difference over the leader, ACC calls for further deceleration, which results in a larger growth.

The indirect effects suggest that growth is smaller if ΔT is larger or Δd_{avg} is smaller, which seem puzzling. Further research is needed for that.

Nevertheless, R3 is interesting as it suggests that amplification is more likely to occur at smaller headway, lower speed, or when the stimulus from the leader is stronger. The impacts can also be observed in the empirical cases as shown in Fig. 16. From Fig. 16(a) to (b), when headway setting increases from 1 to 3, ϕ decreases from 0.26 m/s to 0.44 m/s, illustrating the negative effect. Meanwhile, (c) and (b) shows the effect of speed; i.e., when speed increases from 15.6 m/s to 29.1 m/s, ϕ decreases from 0.53 m/s to 0.44 m/s, illustrating the negative effect. (d) and (a) shows the effect of d_{avg}^L ; i.e., when d_{avg}^L increases from 0.70 m/s² to 1.63 m/s², ϕ increases from 0.05 m/s to 0.26 m/s illustrating the positive effect.

Mechanism of acceleration rate change Δa_{avg}

Per R4-(iii), Δa_{avg} has a negative direct effect from a_{avg}^L . This is expected. During acceleration, ACC has a smaller speed than the leader because of delay. Therefore, when the leader uses a smaller a_{avg}^L , it is easier for ACC to use a similar or even larger acceleration rate than the leader, which results in a larger Δa_{avg} . This will help the ACC to catch up with the leader faster. Note that, at this time, safety is less concerning because ACC speed is smaller than the leader. The ACC could use a smaller acceleration (thus smaller Δa_{avg}) anytime, which will increase spacing faster and favor safety. In other words, it seems that efficacy (i.e., to catch up with the leader) is more likely the driving force for the acceleration behavior.

For the impact of speed and headway per R4 (i) and (ii), since the relationship between speed and the mediator, growth, is already established in R3, the only new component is the positive influence of growth on Δa_{avg} . This can be interpreted as follows. Notice that, at the acceleration start, the speed difference between the leader and follower is larger when ϕ is larger. Particularly, we have observed that at this time stamp, ACC speed is always smaller than the leader. As a result, a larger speed difference motivates ACC to use a stronger acceleration rate to catch up with the leader speed more efficiently (i.e., larger Δa_{avg}). This is aligned with our conjecture that efficacy seems to be the driving force for the acceleration behavior.

Overall, R4 suggests that, ACC will use a larger Δa_{avg} if it has a smaller headway setting, or at a lower speed level, or the leader presents a milder acceleration; see Fig. 16 for the empirical cases: from (a) to (b), headway setting increases from 1 to 3, Δa_{avg} decreases from 0.09 m/s² to -0.15 m/s², illustrating the negative effect. From (c) and (b), speed increases from 15.6 m/s to 29.1 m/s, Δa_{avg} decreases from 0.12 m/s² to -0.15 m/s², illustrating the negative effect. The impacts of a_{avg}^L is not significant in this specific empirical case.

Mechanism of overshooting ψ

R5 suggests that ϕ has a positive influence on ψ . Recall that with a larger growth, the speed difference between the leader and follower is larger when ACC starts the acceleration process. Thus, the ACC spacing level, η , increases faster (i.e., ACC lags behind the leader more) during the acceleration. Theoretically, if ACC can use a very large acceleration to catch up with the leader, then η can increase slowly when recovering to equilibrium and synchronizing the speed with the leader. However, constrained by comfort, ACC cannot use a very strong acceleration. As a result, the spacing level η keeps increasing fast and eventually exceeds the equilibrium, which requires ACC to overshoot to close the excessive spacing and recover. Clearly, larger ϕ demands larger overshoot.

For the impact of Ω , it is fully mediating through ϕ , i.e. larger Ω leads to larger ϕ , which in turn leads to larger ψ . As the second component is just explained above, the positive impact of Ω on ϕ is interpreted as follows. Because of the delay, ACC has a larger speed than the leader at the deceleration process. Thus, the spacing level between ACC and leader, η , keeps decreasing during deceleration. When all other variables are the same, larger Ω means longer deceleration, resulting in larger reduction of η , i.e., ACC approaches closer to the leader at the deceleration end. Therefore ACC decelerates more to reduce the safety risk, and leads to the larger ϕ .

Overall, R5 suggests that, overshooting is more likely to occur at lower speed level and when the leader presents a larger stimulus manifested in Ω . Fig. 16(c) and (b) shows the effect of speed on overshooting; i.e., , as speed increases from 15.6 m/s to 29.1 m/s, ψ decreases from 0.50 m/s to -0.24 m/s, showing the negative effect. The impact of Ω on ψ is shown in Fig. 18(a) and (b). As Ω increases from 2.06 m/s to 3.80 m/s, ψ increases from -0.30 m/s to 0.51 m/s, showing the positive effect.

Summary

Overall, it is found that IVs impact CF behaviors both directly and indirectly. The impact mechanisms for the CF behavior in the deceleration process, including response time (ΔT), deceleration rate change (Δd_{avg}), and growth (ϕ), are mainly driven by safety concern. This is mainly because ΔT is much larger than τ_0 . As a result, ACC has significant safety risks through the deceleration process. Thus, it is not surprising that ΔT has an influence on later ACC behaviors, such as growth ϕ . Moreover, safety becomes a driving force for the ACC behaviors. For the ACC behaviors in the acceleration process (i.e., acceleration rate change, Δa_{avg} , and overshooting, ψ), it is likely that the main driving force is not safety but efficacy - to catch up with the leader and increase the speed faster. Moreover, ACC is likely subject to the comfort constraint (e.g., couldn not use a very large acceleration), which results in excessive spacing and forces ACC to overshoot.

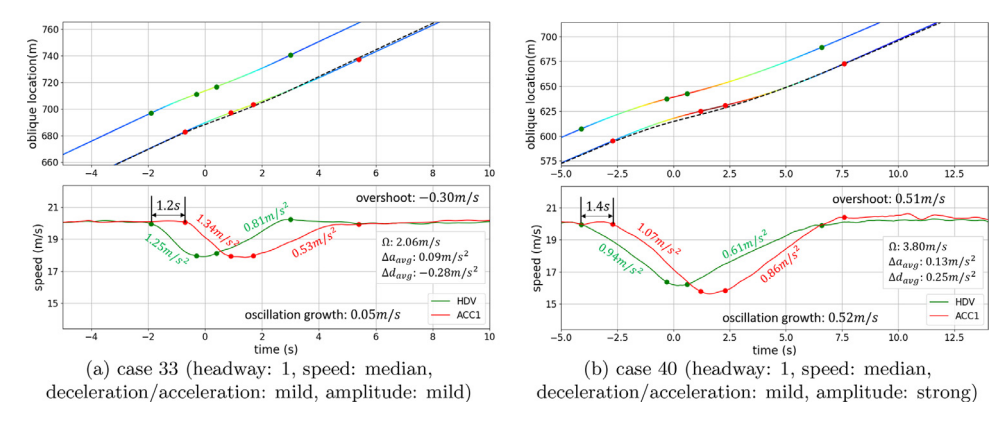


Fig. 18. Empirical cases - different amplitude.

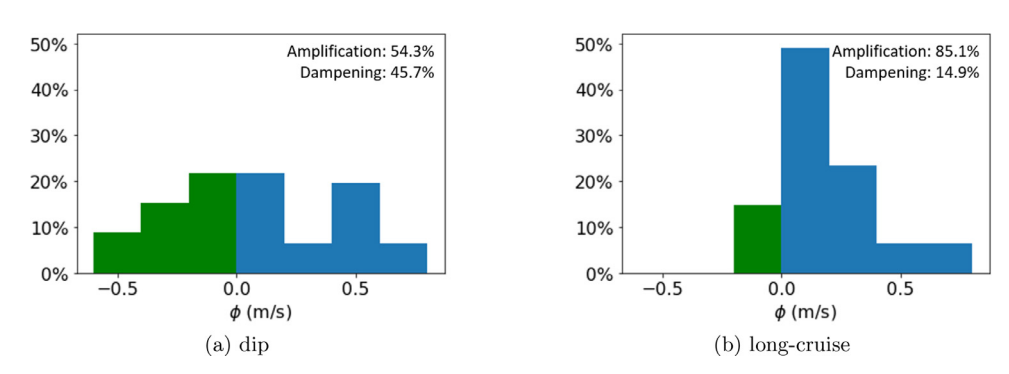


Fig. 19. Distribution of oscillation growth in dip and long-cruise cases in ACC1.

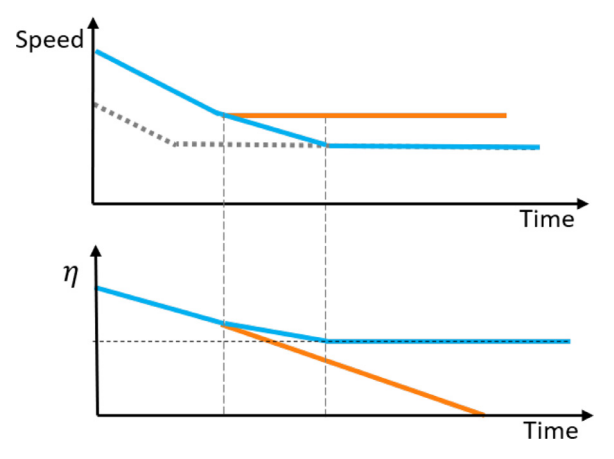


Fig. 20. Dampening in long-cruise.

4.2. Long-cruise cases

This subsection will present the results on long-cruise cases. Note that the deceleration process is identical for the dip and long-cruise cases. Therefore, we will focus on the oscillation growth, acceleration process, and stabilization process. We have conducted a similar analysis as the dip cases using the 47 long-cruise cases.

On oscillation growth (ϕ) , it shows very different features from the dip case (see Fig. 19). An interesting observation is that dampening (i.e., negative ϕ) becomes very rare compared to the significant proportion (45.7%) in the dip case. Note that the very small proportion of negative ϕ (7 cases) are in a mild magnitude (minimum ϕ : 0.08 m/s), comparable to the mean speed measurement error (0.10 m/s) and last momentarily. In fact, persistent dampening is infeasible in the long-cruise case. The distinct features here arise due to the constraint imposed by the long cruising period. An illustrative sketch is provided in Fig. 20. One can see that if the ACC speed maintains a higher speed than the leader in the cruising process, the spacing,

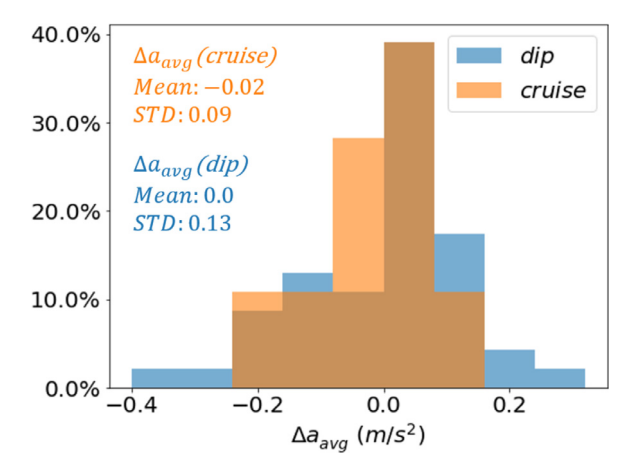


Fig. 21. Distribution of acceleration rate change (Δa_{avg}) in dip and long-cruise cases in ACC1.

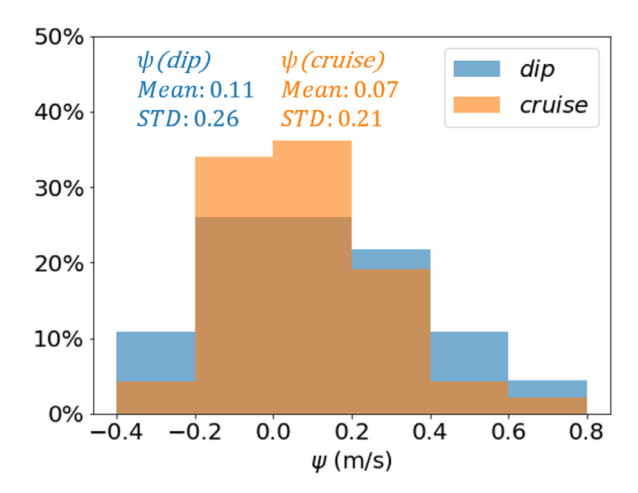


Fig. 22. Distribution of overshooting (ψ) in dip and long-cruise cases in ACC1.

and thus η , keeps decreasing and can lead to a collision; see the orange trajectory. Therefore, at a certain point, ACC has to reduce speed to maintain the minimum tolerable spacing (and η level) to avoid collision (blue trajectory). One can expect that if the cruising period is long enough, eventually the ACC has to decelerate to and stabilize at the leader's speed, which will result in $\phi = 0$. This explains why ACC is very likely to end up with a negligible ϕ and persistent dampening is very rare in our data.

The regression and mediation analysis (see Table B.1 in Appendix B) has shown that, similar to the dip cases, headway and speed both have a negative effect and leader deceleration rate (d_{avg}^L) has a positive effect on ϕ . However, the indirect effects of headway and speed observed in the dip cases are no longer significant.

On the acceleration rate change (Δa_{avg}), the magnitude is smaller than the dip cases and now has a smaller variation; see Fig. 21. Moreover, Δa_{avg} becomes negligible (insignificant from zero) regardless of the headway and speed levels. Regarding the impact factors (Table B.2 in Appendix B), the effects from headway and speed are insignificant, whereas significant negative effects exist in the dip cases. But the leader acceleration rate (a_{avg}^L) still has a direct negative effect, similar to the dip cases.

On the overshooting effect (ψ), the magnitude, be it positive or negative, is smaller than the dip cases and now has a smaller variation; see Fig. 22. Regarding the impact factors (Table B.3 in Appendix B), similar to dip cases, headway has a negligible total effect and speed has a negative effect (but only the direct effect is significant). But, the positive effect from the oscillation amplitude (Ω) observed in dip cases is now insignificant for long-cruise cases.

In summary, compared to the dip cases, in the long-cruise cases, the magnitude of oscillation growth and overshooting/undershooting is much smaller. Also, for the ACC behaviors in the acceleration and stabilization stages of an oscillation, the impacts of IVs are much weaker. For example, the impacts of headway or speed on Δa_{avg} are gone, and so is the impact of Ω on overshooting. Besides, the mediation from earlier ACC behaviors is weaker. For example, the indirect effects from headway and speed on growth are gone.

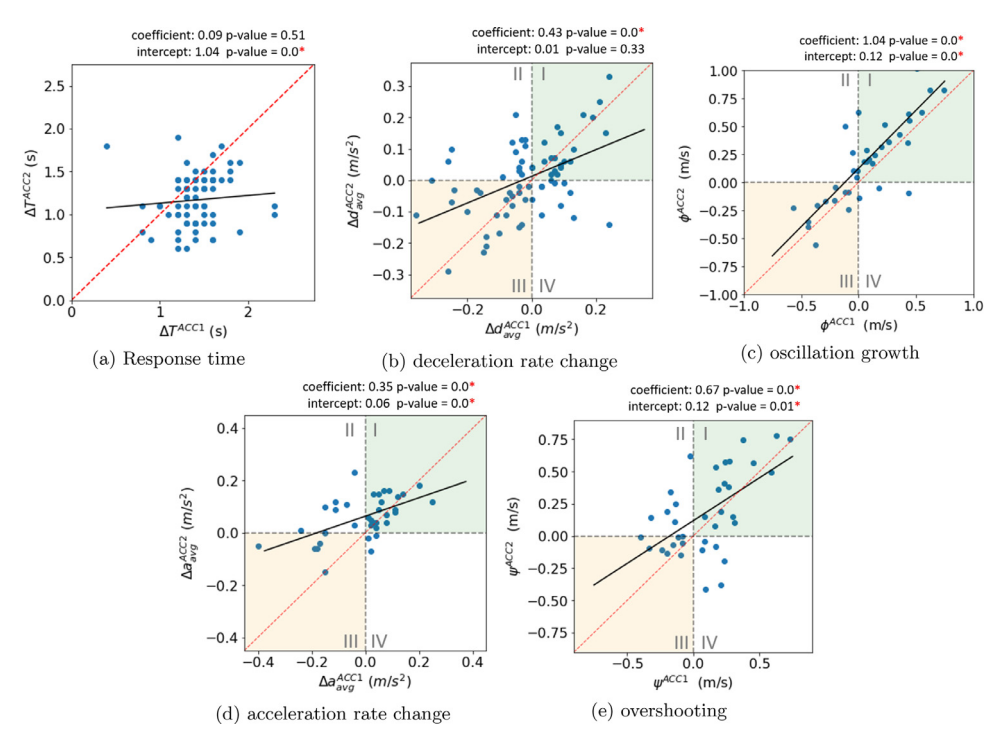


Fig. 23. Behaviors of ACC1 and ACC2.

The difference between the dip and long-cruise cases are expected. In our cases, ACC has been well synchronized with the leader after the long-cruise period. As a result, the acceleration process has very minimum residual effects from the earlier deceleration process; i.e., the mediation effects from earlier ACC behaviors dramatically diminish or even completely disappear.

5. Platoon dynamics

In this section we are interested in the propagation, along a 3-vehicle platoon, of the CF mechanisms described in the previous section. In total, we have 74 oscillation cases (dip and long-cruise) for the platoon analysis.

5.1. Observations on platoon effect

Repeating the same analysis in the previous section with the 2nd ACC in the platoon, whose leader is ACC1, allows us to detect any significant changes in the CF mechanisms. We found that the remarks on the behavior features observed for ACC1 generally hold true for ACC2. But the magnitude of behavior variables can change. Below we briefly introduce the main differences observed on response time, deceleration rate change, oscillation growth, acceleration rate change, and overshooting.

Remark R6: The response time at ACC2 (i) is generally smaller than ACC1; but (ii) the two response time values are not directly correlated. R6 is shown in Fig. 23(a), in which the response time pairs of ACC1 and ACC2 correspond to the same deceleration wave.

Remark R7: The deceleration rate change of ACC2 is positively correlated with ACC1 and shows a regressive effect. Namely, if ACC1 uses a stronger (milder) deceleration than its leader, ACC2 generally does the same; see Fig. 23(b) where 65.2% of the data pairs fall in the first and third quadrant. However, the change magnitude in ACC2 is smaller than ACC1 (the slope of the regression line is 0.43). Notably, the positive correlation suggests that the effect will grow in a platoon, though at a decreasing marginal rate.

Remark R8: The oscillation growth of ACC2 is positively correlated with ACC1 and displays a progressive effect. This is clearly shown in Fig. 23(c).

Remark R9: The acceleration rate change of ACC2 is positively correlated with ACC1 and displays a regressive effect; see Fig. 23(d).

Remark R10: The overshooting effect in ACC2 is positively correlated with ACC1 and displays a regressive effect. This means ACC1 and ACC2 usually both undershooting or overshooting; see Fig. 23(e).

Table 8Estimation results of the MA experiment for the ACC behavior evolution.

Feature	Deceleration rate change	Oscillation growth	Acceleration rate change	Overshooting
Estimated parameters	$\alpha = 0.43, \beta = 0$	$\alpha = 1.04, \beta = 0.12$	$\alpha=0.35,\beta=0.06$	$\alpha = 0.67, \beta = 0.12$

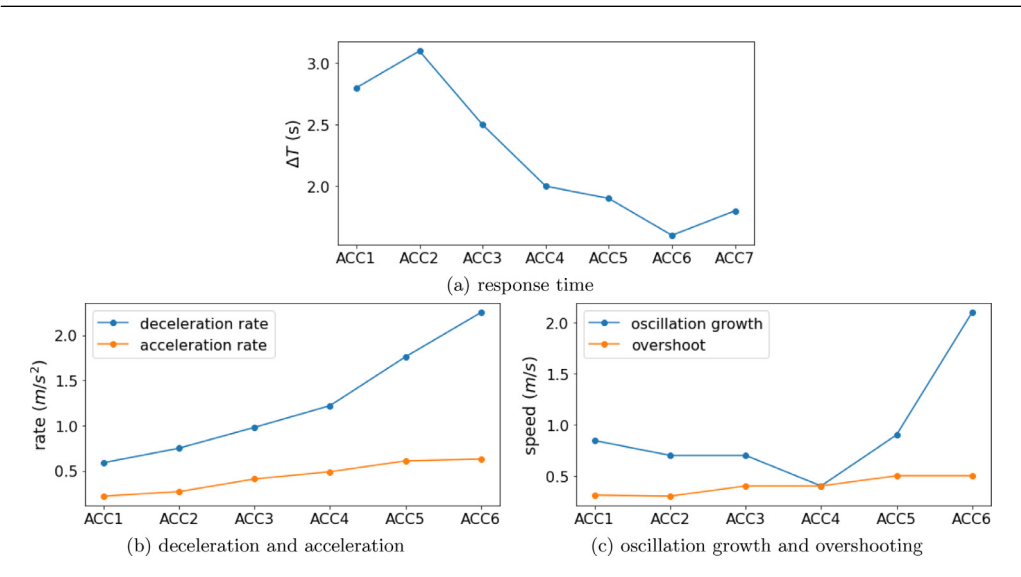


Fig. 24. Evolution of the ACC behaviors in the eight-vehicle platoon.

5.2. Modeling the platoon effect in a multi-vehicle platoon

Remarks R7–R10 suggest that the four CF features may exhibit interesting cumulative effects in a platoon. A first-order approximation for the propagation of a CF effect x (e.g., oscillation growth) can be built as

$$x^n = \alpha x^{n-1} + \beta. \tag{5}$$

where x^n denotes an effect observed for the nth ACC vehicle in the platoon, and α and β denote the coefficients, with $\alpha > 1$ for a progressive effect and $\alpha < 1$ for a regressive effect. Accordingly, we can obtain the cumulative effect for the nth vehicle as

$$x^{n} = \begin{cases} \alpha^{n-1}x^{1} + \beta(1-\alpha^{n-1})/(1-\alpha), & if\alpha \neq 1\\ x^{1} + (n-1)\beta, & if\alpha = 1 \end{cases}$$

$$(6)$$

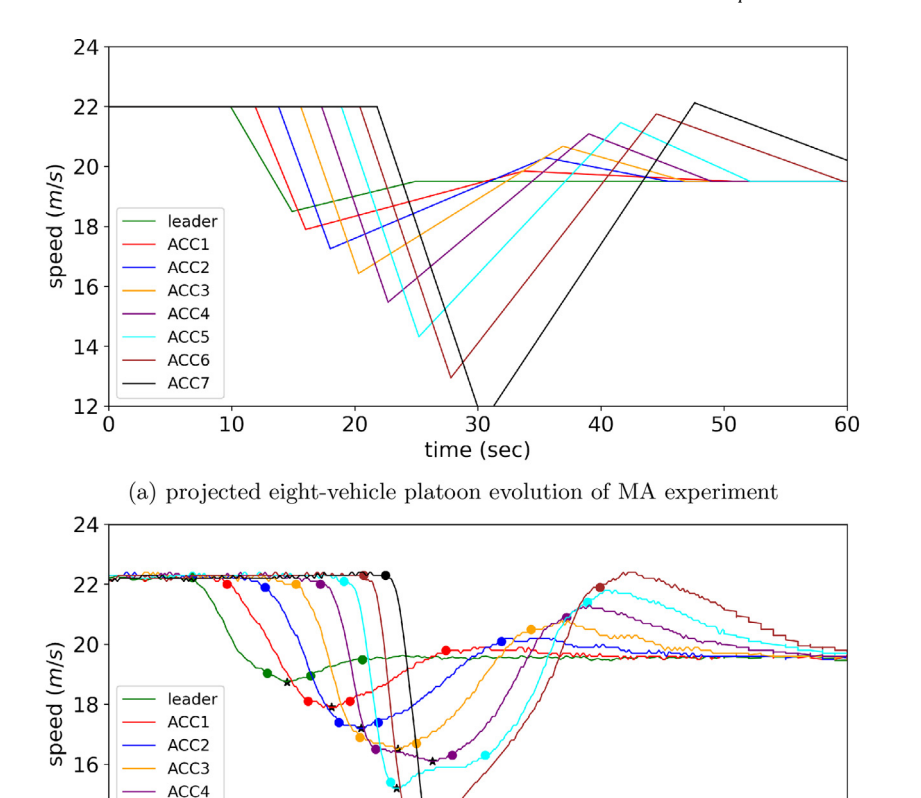
Applying Eq. (5) for each of the four CF features pertaining to remarks (R7–R10), we estimate the growing effect in a single vehicle pair based on our data; see Table 8. Note that the estimated parameters indicate an aggregated outcome. Namely, we have observed varied conditions from the empirical cases (as shown in Fig. 23). For example, the deceleration rate change increases in some cases but decreases in some others. Here, the estimated value represents the average propagation effect.

To validate this approach, we compare the projected platoon effect (using the estimated parameters in Table 8) with the empirical observation of a recent field test conducted by Gunter et al. (2020b) (referred to as the Work experiment), which used seven⁶ identical ACC vehicles from a manufacturer different from the car model X tested in our experiment (referred to as MA experiment).

The extracted CF features from the Work experiment are shown in Fig. 24. In general, the behavior features have a consistent trend with our observations (R6–R10). For example, the response time generally decreases along the platoon (Fig. 24(a)), corresponding well to our remark R6.

We then construct the projected speed profiles of the eight-vehicle platoon based on our first-order model with the estimated parameters per Table 8. Our projection used the same leader profile in the Work experiment. Overall, our projected outcome is qualitatively consistent with the Work experiment; see Fig. 25(a) vs. (b). Both of them show that: (i) the oscillation amplitude exacerbates very quickly (projected outcome: minimum speed is 18.5 m/s for leader and 11.5 m/s for ACC7), (ii) due to the growing effect of deceleration rate, ACC vehicles further upstream have to apply very harsh braking

⁶ There are only effective data for ACC1-ACC6 as ACC7 disengaged during the deceleration process (the driver had to take manual control due to the extreme strength of the deceleration).



(b) empirical eight-vehicle platoon evolution of Work experiment (from Gunter et al. (2020b))

30

time (sec)

40

50

60

20

ACC5

ACC6 ACC7

10

14

12 |

Fig. 25. Projected and empirical speed profiles in a long platoon.

(projected outcome: 0.70 m/s^2 for leader and 1.45 m/s^2 for ACC7), (iii) the acceleration also becomes stronger throughout the platoon (projected outcome: 0.10 m/s^2 for leader and 0.53 m/s^2 for ACC7), and (iv) the growing overshooting effect causes ACC vehicles to significantly exceed the stable speed.

Notably, since the ACC vehicles in the Work experiment were from a car manufacturer different from the car model X, it is surprising how well our first-order and deterministic approximation model is able to capture the propagation of the main ACC behavior features in a long platoon.

6. Discussions

This study has revealed an important message that the CF behaviors of ACC are complex and depend on many factors. Empirical tests are particularly important to understand such complexity. Our results suggest that, aside from simply focusing on ACC stability, detailed analysis helps to better understand how ACC behaves and may further impact the traffic flow. Below we discuss some implications of our findings on traffic flow and controller design.

Recall that ACC response varies with headway setting, speed level, and stimulus. Specifically, amplification and overshooting are more likely to occur when the traffic speed is lower. This implies that, ACC is likely to produce a profound effect in low speed traffic. For example, the increased chance of amplification/overshooting of the ACC may trigger more lane changes of other vehicles, which will then compromise traffic flow efficiency, network capacity, and safety. Besides, our field experience suggests that, even at medium headway (headway-3 for Car Model X), the chance of surrounding vehicle cut-in is high. This implies that, most ACC users probably will use the smaller headway (smaller than headway-3) to avoid cut-in. As a result, the chance of ACC amplification/overshooting is likely high. Moreover, the impacts of stimulus suggest that, if the traffic conditions of a road segment are prone to significant disturbances, ACC is likely to exacerbate that. This contradicts the common claim from car manufacturers that ACC is particularly suitable to handle stop-and-go traffic.

The quantification of ACC impacts on traffic flow is a complex problem and is left for the next paper. Here we provide some thoughts along this line. In addition to the Car Model X, we have tested and analyzed several other ACC systems,

which will be presented in a sequential paper. Our next step is to extrapolate the results from our experiments and other field tests, to the general ACC pool, which will enable us to study the impacts of various ACC systems on traffic flow. We envision that some vehicle features will play a role, such as the engine type, power to weight ratio, and sensing type (e.g., radar vs. Lidar). These will be investigated in future research.

Our findings also provide hints for future controller design. For example, if stability is a concern, the controller design should consider the full spectrum of speed and possible stimulus. To do that, one option is to consider the challenging conditions that are more prone to amplification/overshooting (i.e., low speed, strong deceleration and oscillation amplitude). Another possibility is to parameterize the controller based on the speed levels, which will make it easier to tune a stable controller. Of course, another option is to adjust the headway. For example, the control design can increase the headway to the extent possible to favor stability. But this comes at the cost of compromising the traffic flow throughput.

7. Conclusions

In this paper, we investigated the CF behaviors of ACC vehicles using field experiments with a three-vehicle platoon. Our experiments were designed to examine the ACC response in different conditions with respect to three categories of impact factors, ACC headway setting, traffic speed level, and stimulus from the leader. Based on the data, we have conducted an extensive analysis on the key CF behaviors of ACC throughout an oscillation cycle, including response time, deceleration rate change, oscillation growth, acceleration rate change, and overshooting. Our analysis has revealed the characteristics of these behaviors. Moreover, we have applied the mediation analysis to examine how the three categories of factors impact the ACC behavior and provided our interpretation on the impact mechanisms. Lastly, we have analyzed the propagation of the CF behaviors along a platoon to reveal the platoon effect.

We have found that (i) the ACC response time observed is comparable to human drivers but much larger than the ACC controller time gap and it exhibits small variance, (ii) the ACC response can amplify or dampen an oscillation, (iii) after the oscillation, the stabilization process can exhibit overshooting or undershooting, and (iv) these behaviors depend largely on the ACC headway setting, speed level, and leader stimulus, where the impacts are produced directly and/or indirectly through the mediation of earlier ACC behaviors. For example, headway has a total negative effect on ACC deceleration rate change. Particularly, it has a negative direct effect, and a positive indirect effect mediating through response time, which suppresses the direct effect. Interestingly, the impacts can be well explained from the perspective of safety risk. When the leader profile has a long-cruise period at low speed, ACC displays some unique features. For example, compared to the dip cases, the ACC behaviors in the acceleration and stabilization stages do not heavily depend on headway, speed, and the leader stimulus. The mediation effect from earlier ACC behaviors is much weaker.

From the platoon effect analysis, we have found that the behavior change from one ACC vehicle to the next is progressive for oscillation growth, and regressive for deceleration rate change, acceleration rate change, and overshooting. Based on these observations, we have proposed a simple linear model to capture the growing effects of these CF features in a platoon, whose forecasts are consistent with an empirical 8-vehicle ACC test. The results imply that in long platoons, oscillation amplitude can exacerbate very quickly, which forces ACC vehicles further upstream to apply very strong braking followed by a strong acceleration. This can cause significant overshooting and safety hazards. The good agreement of the linear model with the empirical data was unexpected, and suggests that refinements of this model are worth investigating, such as higher-order approximations and/or adding stochastic components.

This study has several limitations that call for future research. One issue is that, the sample size for the analysis is not very large. It is desirable to have more repetitions of the experiments to improve that. Note that, because of the large number of possible combinations, the needed experiment runs can be prohibitive, but future research can utilize the insights unveiled in this study to optimize the design and minimize the efforts. Another issue is that, due to the limitation in driver execution, the leader deceleration, acceleration, and oscillation amplitude were correlated. Future research is desired to isolate the impact from each of them. This will likely need automated control as the precise control on deceleration/acceleration is very difficult for human drivers.

Future research is also needed to test more ACC car models available in the market so that we can better understand the similarity and difference across different systems. This will help our extrapolation to the general ACC pool. Another issue is that, our analysis of platoon dynamics was built on the data of three-vehicle platoons. A longer platoon is desired to further confirm our findings and calibrate or modify our model. Moreover, future research is desired to study the platoon dynamics with vehicles from different ACC models. For this purpose, the JRC data (Makridis et al., 2020a) is a great starting point, which is under investigation.

CRediT authorship contribution statement

Tienan Li: Conceptualization, Methodology, Data collection, analysis, Writing - original draft. **Danjue Chen:** Conceptualization, Methodology, Writing - review & editing, Funding acquisition, Supervision, Funding acquisition. **Hao Zhou:** Conceptualization, Data collection, Writing - original draft, Writing - review & editing, **Jorge Laval:** Methodology, Funding acquisition, Writing - review & editing, Funding acquisition.

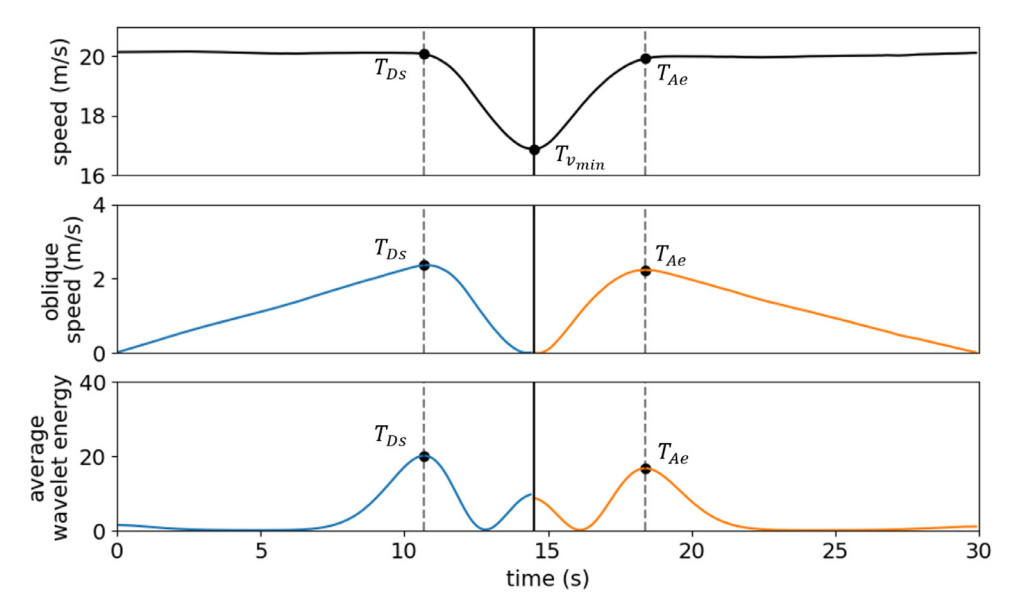


Fig. A1. Recognition $T_{\rm Ds}$ and $T_{\rm Ae}$ using wavelet transform algorithm.

Acknowledgments

This research was sponsored by the National Science Foundation through Awards CMMI 1826162 and CMMI 1932921.

Appendix A. Application of wavelet transform

Fig. A.1 shows an example of the wavelet calculation. Particularly, for the period before $T_{\nu_{min}}$, we first calculate the oblique speed profile to emphasize the singularity (for better recognition performance). T_{Ds} is then captured as the point with the highest average wavelet energy. Similarly, T_{Ae} is the point with the highest energy in the period after $T_{\nu_{min}}$.

Appendix B. Mediation analysis results of long-cruise cases

Table B1 Mediation analysis results on ϕ - long-cruise (mediators: ΔT and Δd_{avg} . total fitting R^2 : 0.542, sample size: 47).

	Impact coefficient		
IV	Indirect	Direct	Total
Headway	0.015	0.122*	0.137*
Speed	0.002	0.011*	0.013*
d_{avg}^{L}	0.010	0.256*	0.266*

Table B2 Mediation analysis results on Δa_{avg} - long-cruise (mediators: ϕ , total fitting R^2 : 0.548, sample size: 47).

	Impact coefficient		
IV	Indirect	Direct	Total
Headway	0.013	0.004	0.010
Speed	0.001	0.002	0.001
a_{avg}^{L}	-	0.284*	0.284*

Table B3 Mediation analysis results on ψ - long-cruise (mediators: ϕ , total fitting R^2 : 0.299, sample size: 47).

	Impact coefficient		
IV	Indirect	Direct	Total
Headway	0.014	0.062	0.076
Speed	0.002	0.018*	0.019*
Ω	0.006	0.011	0.005

Appendix C. List of abbreviations

Table C1 Summary of abbreviations.

Abbreviation	Full name
AB	asymmetric behavior
AV	automated vehicle
ACC	adaptive cruise control
CACC	cooperative adaptive cruise control
CF	car-following
DV	dependent variable
HDV	human-driven vehicle
IV	independent variable
TTC	time-to-collision
JRC	joint research centre

References

Ali, Y., Zheng, Z., Haque, M.M., 2018. Connectivitys impact on mandatory lane-changing behaviour: evidences from a driving simulator study. Transp. Res. Part C 93, 292–309.

Alkim, T.P., Bootsma, G., Hoogendoorn, S.P., 2007. Field operational test "the assisted driver". In: 2007 IEEE Intelligent Vehicles Symposium. IEEE, pp. 1198–1203.

Alter, A.L., Balcetis, E., 2011. Fondness makes the distance grow shorter: desired locations seem closer because they seem more vivid. J. Exp. Soc. Psychol. 47 (1), 16–21.

Bando, M., Hasebe, K., Nakayama, A., Shibata, A., Sugiyama, Y., 1995. Dynamical model of traffic congestion and numerical simulation. Phys. Rev. E 51 (2), 1035

Bu, F., Tan, H.-S., Huang, J., 2010. Design and field testing of a cooperative adaptive cruise control system. In: Proceedings of the 2010 American Control Conference. IEEE, pp. 4616–4621.

Chen, D., Laval, J., Zheng, Z., Ahn, S., 2012. A behavioral car-following model that captures traffic oscillations. Transp. Res. Part B 46 (6), 744-761.

Costa, J., Pinto-Gouveia, J., 2011. The mediation effect of experiential avoidance between coping and psychopathology in chronic pain. Clin. Psychol. Psychother. 18 (1), 34–47.

Fancher, P., 1998. Intelligent Cruise Control Field Operational test. Final report. Volume I: Technical Report. Technical Report.

Graham, M.H., 2003. Confronting multicollinearity in ecological multiple regression. Ecology 84 (11), 2809-2815.

Gunter, G., Gloudemans, D., Stern, R.E., McQuade, S., Bhadani, R., Bunting, M., Delle Monache, M.L., Lysecky, R., Seibold, B., Sprinkle, J., et al., 2020b. Are commercially implemented adaptive cruise control systems string stable? IEEE Trans. Intell. Transp. Syst. doi:10.1109/TITS.2020.3000682.

Gunter, G., Janssen, C., Barbour, W., Stern, R.E., Work, D.B., 2020a. Model-based string stability of adaptive cruise control systems using field data. IEEE Trans. Intell. Veh. 5 (1), 90–99.

Hayes, A.F., 2017. Introduction to Mediation, Moderation, and Conditional Process Analysis: A Regression-Based Approach. Guilford Publications.

Hayward, J.C., 1972. Near-miss determination through use of a scale of danger. Highway Res. Rec. 384, 24-34.

He, Y., Makridis, M., Fontaras, G., Mattas, K., Xu, H., Ciuffo, B., 2020. The energy impact of adaptive cruise control in real-world highway multiple-car-following scenarios. Eur. Transp. Res. Rev. 12, 1–11.

Knoop, V.L., Wang, M., Wilmink, I., Hoedemaeker, D.M., Maaskant, M., der Meer, E.-J.V., 2019. Platoon of sae level-2 automated vehicles on public roads: setup, traffic interactions, and stability. Transp. Res. Rec. 2673 (9), 311–322. doi:10.1177/0361198119845885.

Kyriakidis, M., van de Weijer, C., van Arem, B., Happee, R., 2015. The deployment of advanced driver assistance systems in europe. SSRN 2559034.

Lighthill, M.J., Whitham, G.B., 1955. On kinematic waves I. Flood movement in long rivers. Proc. R. Soc. Lond. Ser. A 229 (1178), 281-316.

Makridis, M., Mattas, K., Anesiadou, A., Ciuffo, B., 2020a. Openacc. an open database of car-following experiments to study the properties of commercial ACC systems. arXiv preprint arXiv:2004.06342

Makridis, M., Mattas, K., Borio, D., Ciuffo, B., 2019. Estimating empirically the response time of commercially available ACC controllers under urban and freeway conditions. In: 2019 6th International Conference on Models and Technologies for Intelligent Transportation Systems (MT-ITS). IEEE, pp. 1–7.

Makridis, M., Mattas, K., Ciuffo, B., 2019. Response time and time headway of an adaptive cruise control. an empirical characterization and potential impacts on road capacity. IEEE Trans. Intell. Transp. Syst. 21 (4), 1677–1686.

Makridis, M., Mattas, K., Ciuffo, B., Re, F., Kriston, A., Minarini, F., Rognelund, G., 2020. Empirical study on the properties of adaptive cruise control systems and their impact on traffic flow and string stability. Transp. Res. Rec. 2674 (4), 471–484.

Milanés, V., Shladover, S.E., 2014. Modeling cooperative and autonomous adaptive cruise control dynamic responses using experimental data. Transp. Res. Part C 48, 285–300.

Milanés, V., Shladover, S.E., Spring, J., Nowakowski, C., Kawazoe, H., Nakamura, M., 2013. Cooperative adaptive cruise control in real traffic situations. IEEE Trans. Intell. Transp. Syst. 15 (1), 296–305.

Naus, G.J., Ploeg, J., Van de Molengraft, M., Heemels, W., Steinbuch, M., 2010. Design and implementation of parameterized adaptive cruise control: an explicit model predictive control approach. Control Eng. Pract. 18 (8), 882–892.

Naus, G.J., Vugts, R.P., Ploeg, J., van De Molengraft, M.J., Steinbuch, M., 2010. String-stable CACC design and experimental validation: a frequency-domain approach. IEEE Trans. Veh. Technol. 59 (9), 4268–4279.

Newell, G.F., 2002. A simplified car-following theory: a lower order model. Transp. Res. Part B 36 (3), 195-205.

Ozaki, H., 1993. Reaction and anticipation in the car-following behavior. In: Proceeding of 12th International Symposium on Theory of Traffic Flow and Transportation, pp. 349–366.

Ploeg, J., Scheepers, B.T., Van Nunen, E., Van de Wouw, N., Nijmeijer, H., 2011. Design and experimental evaluation of cooperative adaptive cruise control. In: 2011 14th International IEEE Conference on Intelligent Transportation Systems (ITSC). IEEE, pp. 260–265.

Preacher, K.J., Hayes, A.F., 2004. SPSS and SAS procedures for estimating indirect effects in simple mediation models. Behav. Res. Methods Instrum. Comput. 36 (4), 717–731.

Richards, P.I., 1956. Shock waves on the highway. Oper. Res. 4 (1), 42-51.

Ruby, M.B., Dunn, E.W., Perrino, A., Gillis, R., Viel, S., 2011. The invisible benefits of exercise.. Health Psychol. 30 (1), 67.

Schakel, W.J., Gorter, C.M., de Winter, J.C., van Arem, B., 2017. Driving characteristics and adaptive cruise control? A naturalistic driving study. IEEE Intell. Transp. Syst. Mag. 9 (2), 17–24.

Sharma, A., Zheng, Z., Bhaskar, A., 2019. Is more always better? The impact of vehicular trajectory completeness on car-following model calibration and validation. Transp. Res. Part B 120, 49–75.

Tian, J., Zhang, H., Treiber, M., Jiang, R., Gao, Z.-Y., Jia, B., 2019. On the role of speed adaptation and spacing indifference in traffic instability: evidence from car-following experiments and its stochastic model. Transp. Res. Part B 129, 334–350.

Viti, F., Hoogendoorn, S.P., Alkim, T.P., Bootsma, G., 2008. Driving behavior interaction with ACC: results from a field operational test in the netherlands. In: 2008 IEEE Intelligent Vehicles Symposium. IEEE, pp. 745–750.

Wikipedia, 2020. Adaptive cruise control.

Zheng, Z., Ahn, S., Chen, D., Laval, J., 2011. Applications of wavelet transform for analysis of freeway traffic: bottlenecks, transient traffic, and traffic oscillations. Transp. Res. Part B 45 (2), 372–384.

Zhou, Y., Ahn, S., 2019. Robust local and string stability for a decentralized car following control strategy for connected automated vehicles. Transp. Res. Part B 125, 175–196.